

# GPU-Accelerated Loopy Belief Propagation for Program Analysis

Haoyu Feng  
 Peking University  
 haoyufeng@stu.pku.edu.cn

Xin Zhang  
 Peking University  
 xin@pku.edu.cn

September 29, 2025

## Abstract

Loopy Belief Propagation (LBP) is a widely used approximate inference algorithm in probabilistic graphical models, with applications in computer vision, error correction codes, protein folding, program analysis, etc. However, LBP faces significant computational challenges when applied to large-scale program analysis. While GPU (Graphics Processing Unit) parallel computing provides a promising solution, existing approaches lack support for flexible update strategies and have yet to integrate logical constraints with GPU acceleration, leading to suboptimal practical performance.

This paper presents a GPU-accelerated LBP algorithm for program analysis. To support the diverse update strategies required by users, we propose a unified representation for specifying arbitrary user-defined update strategies, along with a dependency analysis algorithm. Furthermore, building on previous work that leverages the local structure of Horn clauses to simplify message passing, we group messages to minimize warp divergence and better utilize GPU resources. Experimental results on datarace analysis over eight real-world Java programs show that our approach achieves an average speedup of  $2.14\times$  over the state-of-the-art sequential approach and  $5.56\times$  over the state-of-the-art GPU-based approach, while maintaining high accuracy.

## 1 introduction

Loopy Belief Propagation (LBP) is a widely used approximate inference algorithm for probabilistic graphical models [26]. In such models, random variables are represented as vertices, and their dependencies are captured by edges. Inference is typically performed via message passing mechanism. Exact inference algorithms are often computationally intractable in practice due to high complexity, making approximate algorithms more practical. LBP is a prominent approximate inference algorithm [23] that operates iteratively on the graphical model, during which each edge collects messages from its neighboring edges to compute a new outgoing message. This process repeats until convergence or for a certain number of iterations, yielding an approximate solution. Due to its simplicity and efficiency, LBP has been successfully applied in diverse fields including computer vision [12], error-correcting codes [19], protein folding [34], program analysis [27], etc.

In recent years, the combination of logic programming and probabilistic reasoning has led to broader applications of LBP in program analysis [27, 6, 35, 37, 32]. These approaches attach probabilities to logical rules in Datalog program analysis, transform the analysis results into probabilistic graphical models, and then perform inference to obtain probabilities of analysis outcomes. For instance, the BINGO framework [27] converts the Datalog program analysis into a directed acyclic graph, transform the graph into a Bayesian network, and applies LBP for Bayesian inference. The resulting bug reports are ranked by their probabilities of being true and presented to the user. User feedback is then incorporated as evidence to update the model and re-rank the reports iteratively. This interactive process enables users to detect a large number of program bugs while inspecting only a small subset of reports. Thus, LBP plays a critical role in such program analysis systems. Given its wide applicability and growing potential in program analysis, improving the efficiency of the LBP algorithm is of significant importance.

However, program analysis on large-scale software often results in large probabilistic graphical models, leading to high computation cost for LBP. Table 1 shows the scale of probabilistic graphical models derived from a datarace analysis on eight real-world Java programs [27]. As shown, the number of vertices and edges ranges from hundreds to hundreds of thousands. Since LBP requires iterative message passing over every edge, this scale severely limits its computational speed.

Table 1: Scale of probabilistic graphical models from a datarace analysis on eight Java programs

Program	weblech	hedc	luindex	jspider	avrora	xalan	sunflow	ftp
KLOC	322	292	299	298	318	495	529	305
# Vertices	696	5,347	11,857	25,162	36,091	51,820	156,695	211,175
# Edges	1,655	14,231	29,237	74,201	100,789	146,334	431,497	476,915

A common approach to handling the computational cost of LBP on large-scale models is to leverage the high performance of GPUs (Graphics Processing Units). The message passing computations in LBP involve numerous independent operations with uniform computation patterns, making the algorithm highly suitable for GPU acceleration. With rapid advancements in GPU technology and growing research interest, GPUs have been widely adopted to improve LBP performance [15, 5, 28, 38]. However, GPU-based parallel LBP algorithms tailored for program analysis remain unexplored. Existing GPU implementations designed for domains such as computer vision [15, 5] and error-correcting codes [28] often support only specific graph structures and domain-specific update strategies, and fail to exploit logical constraints inherent in program analysis. General-purpose GPU implementations [38], while supporting arbitrary graph structures, employ simple update strategies that fall short of real-world requirements and similarly ignore domain-specific logical constraints. This paper aims to address these limitations and fill the gap in GPU-accelerated LBP for program analysis.

This paper presents a GPU-accelerated LBP algorithm specifically designed for program analysis. First, in program analysis applications, LBP update strategies are often flexible and may vary according to user needs. For example, users would expect messages on all edges to be updated simultaneously when prioritizing speed over accuracy, or topological-order updates for trees. We propose a unified representation for user-specified update strategies and introduce a algorithm to analyze their dependency relationships, enabling effective parallelization of message updates. Second, the logic rules used in program analysis are typically Horn clauses of the form  $x_1 \wedge \dots \wedge x_n \rightarrow y$ . The probabilistic graphical models derived from such rules exhibit specific local structures [8]. While Wu et al. [31] proposed exploiting this structure to reduce computational complexity, their approach changes the message passing procedure. We leverage the SIMD (Single Instruction, Multiple Data) architecture of GPUs by grouping different types of message computations to minimize thread divergence and maximize GPU utilization.

We conduct extensive experiments to evaluate the efficiency and accuracy of our algorithm. We implement the proposed algorithm in a prototype system and compare it with state-of-the-art approaches [31, 38]. Our evaluation uses the same eight real-world Java programs (ranging from 292 to 529 KLOC) as prior work [27] for datarace analysis. Experimental results show that: (1) compared to the state-of-the-art sequential method [31], our approach achieves an average speedup of  $2.14\times$  while maintaining the accuracy; (2) compared to the state-of-the-art GPU-based method [38], our approach achieves an average speedup of  $5.56\times$ , also preserving accuracy.

In summary, our contributions are as follows:

- We propose a unified representation for user-defined update strategies and a method to analyze their dependencies for effective parallelization.
- We present a GPU-parallel LBP algorithm tailored for probabilistic graphical models derived from Horn clauses.
- We implement a high-performance prototype system and conduct experiments to validate the efficiency and accuracy of our approach.

## 2 Preliminaries

Before introducing our approach, we provide a brief overview of Loopy Belief Propagation, Bayesian program analysis, and the application of Loopy Belief Propagation in Bayesian program analysis. For more detailed treatments, we refer the reader to books [8, 1, 16] and papers [27, 31].

### 2.1 Loopy Belief Propagation

Loopy Belief Propagation (LBP) is a common approximate inference algorithm for probabilistic graphical models. It operates by iteratively passing messages on a factor graph, terminates when certain conditions

are met, and finally computes the marginal distributions of random variables. This subsection introduces, in order, the definition of factor graphs, the mechanism of message passing, and the method for computing marginal distributions.

A factor graph is a special type of probabilistic graphical model. Common models such as Bayesian networks and Markov random fields can be converted into factor graphs, enabling a unified approach to inference. In particular, LBP is an inference algorithm running on factor graphs. We now formally define factor graphs.

**Definition 2.1** (Factor Graph). Given a set of random variables  $\mathbf{X} = \{X_1, X_2, \dots, X_n\}$ <sup>1</sup>, suppose their joint probability distribution can be factorized into a product of functions:

$$P(\mathbf{X}) = \frac{1}{Z} \prod_{a \in A} f_a(\mathbf{X}_a),$$

where:  $\mathbf{X}_a \subseteq \mathbf{X}$  is a subset of  $\mathbf{X}$ ,  $f_a : \bar{X}_a \rightarrow \mathbb{R}_{\geq 0}$  is a non-negative function, and  $Z$  is the normalization constant.

The corresponding factor graph is represented as a pair consisting of a bipartite graph and  $\mathbf{X}$ :

$$FG = ((V, A, E), \mathbf{X}),$$

where:  $V = \{v_1, v_2, \dots, v_n\}$  is the set of variable nodes, each node  $v_i$  corresponding to the random variable  $X_i$ ;  $A = \{a_1, a_2, \dots, a_m\}$  is the set of factor nodes, each node  $a_j$  corresponding to the function  $f_{a_j}$ ; and  $E \subseteq V \times A$  is the set of edges, such that an edge  $(v_i, a_j) \in E$  exists if and only if  $X_i \in \mathbf{X}_{a_j}$ .

Note: For notational convenience, in this paper we use both the node index and the node symbol as subscripts for the corresponding random variable. For example,  $X_i$  and  $X_{v_i}$  both denote the random variable associated with node  $v_i$ . The appropriate form will be used depending on context in the following text.

A message is a mapping from the values of a random variable to non-negative real numbers. Each edge corresponds to two messages: one from a variable to a factor and another from a factor to a variable. Message passing refers to the process of computing new messages based on messages from neighboring edges. Below, we formally define message passing using the sum-product algorithm [17].

**Definition 2.2** (Message Passing). Given a factor graph  $FG = ((V, A, E), \mathbf{X})$ , for any  $v \in V$  and  $a \in A$ , the message from a variable to a factor  $\mu_{v \rightarrow a} : \bar{X}_v \rightarrow \mathbb{R}_{\geq 0}$  is defined as:

$$\mu_{v \rightarrow a}(x_v) = \prod_{a^* \in N_V(v) \setminus \{a\}} \mu_{a^* \rightarrow v}(x_v), \quad (1)$$

and the message from a factor to a variable  $\mu_{a \rightarrow v} : \bar{X}_v \rightarrow \mathbb{R}_{\geq 0}$  is defined as:

$$\mu_{a \rightarrow v}(x_v) = \sum_{\mathbf{x}_a \setminus x_v} f_a(\mathbf{x}_a) \prod_{v^* \in N_A(a) \setminus \{v\}} \mu_{v^* \rightarrow a}(x_{v^*}), \quad (2)$$

where:  $x_v \in \bar{X}_v$ ,  $x_{v^*} \in \bar{X}_{v^*}$ ,  $\mathbf{x}_a \in \bar{\mathbf{X}}_a$ , and  $\sum_{\mathbf{x}_a \setminus x_v}$  denotes summation over all possible values of  $\mathbf{x}_a$  while keeping  $x_v$  fixed;  $N_V : V \rightarrow \mathcal{P}(A)$  represents the set of factors adjacent to a variable, i.e.,  $\forall v \in V, N_V(v) = \{a | (v, a) \in E\}$ ;  $N_A : A \rightarrow \mathcal{P}(V)$  represents the set of variables adjacent to a factor, i.e.,  $\forall a \in A, N_A(a) = \{v | (v, a) \in E\}$ . Additionally, if  $N_V(v) = \{a\}$  or  $N_A(a) = \{v\}$ , the corresponding product in the above definitions is taken to be 1.

Given a vertex  $v \in V$ , its exact or approximate marginal distribution can be computed as:

$$P(X_v = x_v) = \frac{\prod_{a \in N_V(v)} \mu_{a \rightarrow v}(x_v)}{\sum_{x_v \in \bar{X}_v} \prod_{a \in N_V(v)} \mu_{a \rightarrow v}(x_v)}. \quad (3)$$

After all messages are initialized, they are updated iteratively according to Equations (1) and (2). For chain-structured or tree-structured factor graphs, the iterations are guaranteed to converge, and the result from Equation (3) gives the exact marginal distribution. However, for factor graphs with loops, convergence is not guaranteed. Nevertheless, iterative computation can still be performed and terminated after a fixed amount of time or a certain number of iterations. In such cases, the result from Equation (3)

---

<sup>1</sup>In this paper,  $\bar{X}$  denotes the domain of the random variable  $X$ .

serves as an approximation. This method is known as **Loopy Belief Propagation**. We omit the relevant theoretical proofs here. It is worth noting that Definition 2.2 does not specify whether messages should be computed based on values from the current iteration or the previous one. In practice, the choice of update schedule—such as synchronous, asynchronous, or priority-based updating—can significantly affect both convergence behavior and final accuracy. We will discuss update strategies in greater detail in later sections.

## 2.2 Bayesian Program Analysis

This subsection provides a brief introduction to Bayesian program analysis, which serves as the primary application scenario for our method. Bayesian program analysis attaches probabilities to logical rules in Datalog-based program analyses, transforms the analysis results into a Bayesian network, and then performs inference on the network to obtain probabilistic estimates of the outcomes. If the truth values of some random variables are known—such as from user feedback—these variables can be treated as evidence in the Bayesian network, leading to more accurate posterior probabilities in subsequent inference. For example, the BINGO framework [27] uses the probabilities derived from Bayesian inference to rank bug reports and presents them to users. These reports may be true positives or false positives. Users inspect the highest-ranked reports that are most likely to be true and label them as true or false. These labels are then fed back into the Bayesian network as evidence, enabling an interactive refinement process that aims to uncover as many true bugs as possible with minimal inspection effort.

The rest of this subsection first reviews Datalog and Bayesian networks, and then explains how to transform a Datalog program analysis into a Bayesian network.

	$\llbracket C \rrbracket = \text{lfp } F_C \in \mathcal{P}(\mathbf{T})$
(Program)	$C ::= c^*$
(Constraint)	$c ::= l : -l^*$
(Literal)	$l ::= r(a^*)$
(Argument)	$a ::= v \mid d$
(Variables)	$v \in \mathbf{V} = \{x, y, \dots\}$
(Constants)	$d \in \mathbf{D} = \{0, 1, \dots\}$
(Relations)	$r \in \mathbf{R} = \{r_1, r_2, \dots\}$
(Tuples)	$t \in \mathbf{T} = \mathbf{R} \times \mathbf{D}^*$
(Inputs)	$i \in \mathbf{I} \subseteq \mathbf{T}$
	$F_C(T) = T \cup \bigcup_{c \in C} f_c(T)$
	$f_{l_0: -l_1, \dots, l_n}(T) = \{g_{l_0}(\sigma) \mid \exists \sigma \in \mathbf{V} \rightarrow \mathbf{D}\}$
	$g_{l_k}(\sigma) \in T \text{ for } 1 \leq k \leq n\}$
	$g_{r(a_1, \dots, a_n)}(\sigma) = r(\text{sub}(a_1), \dots, \text{sub}(a_n)),$
	where $\text{sub}(a_i) = \begin{cases} a_i, & a_i \in \mathbf{D}, \\ \sigma(a_i), & a_i \in \mathbf{V}. \end{cases}$

(a) Syntax of Datalog.

(b) Semantics of Datalog.

Figure 1: Syntax and semantics of Datalog.  $*$  denotes zero or more matches.

**Syntax and Semantics of Datalog.** Datalog is a logic programming language widely used as a specification language for program analysis. Figure 1a shows the syntax of Datalog. A Datalog program  $C$  consists of a set of constraints. Each constraint  $c \in C$  has a head literal and a body consisting of a set of literals, representing the conclusion and premises of the rule, respectively. A literal comprises a relation  $r \in \mathbf{R}$  and a sequence of arguments, each of which is either a variable or a constant. A literal with all-constant arguments is called a tuple. The input to a program is a set of tuples  $\mathbf{I}$ .

Figure 1b presents the semantics of Datalog. A Datalog program  $C$  computes its output as the least fixed point (lfp) starting from the input set of tuples  $\mathbf{I}$ . Each constraint encodes the following inference rule: if there exists a substitution  $\sigma : \mathbf{V} \rightarrow \mathbf{D}$  such that, when applied to all variables in the body literals, each resulting ground literal is present in the current set of known tuples, then the head literal, after applying  $\sigma$ , is added to the output. The least fixed point is computed by iteratively applying this rule to all constraints—starting from the input set  $\mathbf{I}$  as the initial known set, generating new tuples, and repeating the process with the updated set until no new tuples are produced. The final result is the set of output tuples  $\llbracket C \rrbracket$ .

**Bayesian Networks.** A Bayesian network is a probabilistic graphical model that represents a set of random variables and their conditional dependencies via a directed acyclic graph (DAG). The nodes in

the graph represent random variables, and the directed edges represent conditional dependencies between them. Below, we formally define a Bayesian network.

**Definition 2.3** (Bayesian Network). A Bayesian network can be represented as a pair:

$$BN = (G, \mathbf{X}),$$

where:  $G = (V, E)$  is a directed acyclic graph, with  $V = \{v_1, v_2, \dots, v_n\}$  being the set of nodes and  $E \subseteq V \times V$  the set of directed edges;  $\mathbf{X} = \{X_1, X_2, \dots, X_n\}$  is a set of random variables, each  $X_i$  associated with node  $v_i$ , and the joint probability distribution over  $\mathbf{X}$  factorizes into a product of conditional probability distributions:

$$P(\mathbf{X}) = \prod_{v \in V} P(X_v | \mathbf{X}_{\text{Pa}(v)}),$$

where  $\text{Pa}(v) = \{u \in V \mid (u, v) \in E\}$ ,  $\mathbf{X}_{\text{Pa}(v)} = \{X_u \in \mathbf{X} \mid u \in \text{Pa}(v)\} \subseteq \mathbf{X}$ ,  $\forall v \in V$ .

**From Datalog Program Analysis to Bayesian Networks.** The process of deriving a fixed point from a Datalog program yields a directed graph. First, the set of conclusions is initialized as  $\llbracket C \rrbracket := \mathbf{I}$  and the set of grounded constraints as  $GC := \{\text{True} \Rightarrow i \mid i \in \mathbf{I}\}$ , using the input set  $\mathbf{I}$ . Then, the fixed point is computed: for any constraint  $l_0 : -l_1, \dots, l_n$ , if there exists a substitution  $\sigma \in \mathbf{V} \rightarrow \mathbf{D}$  such that  $g_{l_1}(\sigma), \dots, g_{l_n}(\sigma) \in \llbracket C \rrbracket$ , the conclusions are updated as  $\llbracket C \rrbracket := \llbracket C \rrbracket \cup \{g_{l_0}(\sigma)\}$  and the grounded constraints are updated as  $GC := GC \cup \{g_{l_1}(\sigma) \wedge \dots \wedge g_{l_n}(\sigma) \Rightarrow g_{l_0}(\sigma)\}$ . The directed graph  $G = (V, E)$  is called a **derivation graph** if  $V = \llbracket C \rrbracket \cup GC$ , there are no edges between vertices in  $\llbracket C \rrbracket$  or within  $GC$ , an edge exists from a vertex  $t \in \llbracket C \rrbracket$  to  $g \in GC$  if and only if  $t$  is a premise of  $g$ , and an edge exists from  $g$  to  $t$  if and only if  $t$  is the conclusion of  $g$ .

The directly generated derivation graph may contain cycles. To convert it into a Bayesian network, it must first be transformed into an acyclic graph. The BINGO framework provides a cycle elimination algorithm that obtains an acyclic subgraph while preserving the conclusions  $\llbracket C \rrbracket$ . Then, an optimization algorithm is applied to compress chain-like structures in the graph, reducing its size without affecting the relations of interest to the user. These algorithms have achieved good performance in practice. Details can be found in paper [27].

Once the DAG is obtained, probabilities need to be attached to form a Bayesian network. Assume that each vertex's corresponding random variable follows a Bernoulli distribution<sup>2</sup>, as we are only concerned with whether tuples or derivations hold true or not. Each grounded constraint  $g \in GC$  is a Horn clause of the form  $g = (t_1 \wedge \dots \wedge t_n \Rightarrow t_0)$ . Since the analysis is an over-approximation, if all premises hold, there is some probability that the conclusion holds; however, if any premise does not hold, the conclusion will definitely not hold. Let  $p$  be the probability that the constraint holds, then in the Bayesian network we have:

$$\begin{aligned} P(X_g = 1 \mid (\bigwedge_{i=1}^n X_{t_i}) = 1) &= p, & P(X_g = 0 \mid (\bigwedge_{i=1}^n X_{t_i}) = 1) &= 1 - p, \\ P(X_g = 1 \mid (\bigwedge_{i=1}^n X_{t_i}) = 0) &= 0, & P(X_g = 0 \mid (\bigwedge_{i=1}^n X_{t_i}) = 0) &= 1. \end{aligned} \tag{4}$$

Specifically, for grounded constraints of the form  $g = (\text{True} \Rightarrow t_0)$ , in the Bayesian network we have:

$$P(X_g = 1) = p, \quad P(X_g = 0) = 1 - p. \tag{5}$$

Each tuple  $t \in \llbracket C \rrbracket$  can be derived from multiple different grounded constraints  $\text{Pa}(t)$ . For any tuple, it can be derived from at least one concrete constraint according to the fixed point computation process. Specifically, for input tuples  $i \in \mathbf{I}$ , there is always a constraint  $\text{True} \Rightarrow i$ . Therefore, for any tuple  $t$ ,  $\text{Pa}(t) \neq \emptyset$ . In the Bayesian network, we have:

$$\begin{aligned} P(X_t = 1 \mid (\bigvee_{g \in \text{Pa}(t)} X_g) = 1) &= 1, & P(X_t = 0 \mid (\bigvee_{g \in \text{Pa}(t)} X_g) = 1) &= 0, \\ P(X_t = 1 \mid (\bigvee_{g \in \text{Pa}(t)} X_g) = 0) &= 0, & P(X_t = 0 \mid (\bigvee_{g \in \text{Pa}(t)} X_g) = 0) &= 1. \end{aligned} \tag{6}$$

<sup>2</sup>In this paper, we use 1 to denote that the random variable is true and 0 to denote false

When sufficient training data is available,  $p$  can be estimated using statistical counting or the Expectation Maximization (EM) algorithm [16]. However, in practice, sufficient training data is often unavailable. So for simplicity, all  $p$  values can be set to a fixed value, such as 0.999, which still yields good results.

So far, we have constructed a Bayesian network from a Datalog program analysis. The next step is to compute the marginal distributions of the random variables. Specifically, for any random variable  $X \in \mathbf{X}$ , we aim to compute  $P(X)$  in the absence of evidence, and  $P(X | \mathbf{X}_e)$  when evidence  $\mathbf{X}_e \subseteq \mathbf{X}$  is given. In this paper, we use LBP to perform this inference.

### 2.3 Loopy Belief Propagation in Bayesian Program Analysis

This subsection introduces how to compute marginal distributions of random variables in Bayesian program analysis using LBP. We first present the transformation of a Bayesian network into a factor graph, and then describe the message passing optimization method proposed by Wu et al. [31].

To perform LBP, the Bayesian network must first be converted into a factor graph. As can be seen from Definition 2.1 and Definition 2.3, a factor graph corresponding to a Bayesian network can be obtained by mapping each (conditional) probability distribution to a factor function. Table 2 presents two more general factor functions.<sup>3</sup> The “AND” factor in Table 2a corresponds to the conditional probabilities represented by Equations (4) and (5). When  $p_1 = p$  and  $p_2 = 0$ , the “AND” factor corresponds to Equation (4). By additionally defining the case  $n = 0$  such that  $p_1 = p_2$ , when  $n = 0$  and  $p_1 = p_2 = p$ , the “AND” factor corresponds to Equation (5). When  $p_1 = 1$  and  $p_2 = 0$ , the “OR” factor in Table 2b corresponds to the conditional probability described by Equation (6). Suppose a variable  $v_e$  is observed to be true or false; the way to incorporate evidence is to connect an additional “AND” factor to  $v_e$ , setting  $n = 0$  and  $p_1 = p_2 = 0$  or 1, respectively. LBP can then be used to compute the posterior probabilities given the evidence. In general, the method presented in this paper is not limited to the conditional probabilities shown in Section 2.2; it applies to any scenario where the factors can be expressed using the forms in Table 2.

Table 2: Factor functions corresponding to conditional probabilities

(a) “AND” factor		(b) “OR” factor	
Input values	Function value	Input values	Function value
$(\bigwedge_{i=1}^n x_i) = 1, x_0 = 1$	$p_1$	$(\bigvee_{i=1}^n x_i) = 1, x_0 = 1$	$p_1$
$(\bigwedge_{i=1}^n x_i) = 1, x_0 = 0$	$1 - p_1$	$(\bigvee_{i=1}^n x_i) = 1, x_0 = 0$	$1 - p_1$
$(\bigwedge_{i=1}^n x_i) = 0, x_0 = 1$	$p_2$	$(\bigvee_{i=1}^n x_i) = 0, x_0 = 1$	$p_2$
$(\bigwedge_{i=1}^n x_i) = 0, x_0 = 0$	$1 - p_2$	$(\bigvee_{i=1}^n x_i) = 0, x_0 = 0$	$1 - p_2$

Next, based on Table 2, we introduce the message-passing optimization method proposed by Wu et al. [31]. Since the original paper does not provide detailed computation processes, we will thoroughly illustrate these steps as a supplement. Let  $a$  denote a factor, and let  $N_A(a) = \{v_0, v_1, \dots, v_n\}$  represent the set of neighboring variable vertices corresponding to variables  $x_0, x_1, \dots, x_n$  in Table 2. We define  $\mathbf{x} = (x_1, \dots, x_n)$  and let  $f_a(x_0, \mathbf{x})$  or  $f_a(x_0, x_1, \dots, x_n)$  be the function associated with factor  $a$ . Considering

<sup>3</sup>Note: The  $n$  and subscripts in this table have different meanings from those in Definition 2.1

the “AND” factor, for each  $v_j \in N_A(a) \setminus \{v_0\}$ , from Equations (2) and Table 2a, we have:

$$\begin{aligned}
\mu_{a \rightarrow v_j}(1) &= \sum_{x_0} \sum_{\mathbf{x} \setminus \{x_j\}} f_a(x_0, \dots, x_{j-1}, 1, x_{j+1}, x_n) \prod_{\substack{i=0 \\ i \neq j}}^n \mu_{v_i \rightarrow a}(x_i) \\
&= \mu_{v_0 \rightarrow a}(0) \sum_{\mathbf{x} \setminus \{x_j\}} f_a(0, \dots, x_{j-1}, 1, x_{j+1}, x_n) \prod_{\substack{i=1 \\ i \neq j}}^n \mu_{v_i \rightarrow a}(x_i) \\
&\quad + \mu_{v_0 \rightarrow a}(1) \sum_{\mathbf{x} \setminus \{x_j\}} f_a(1, \dots, x_{j-1}, 1, x_{j+1}, x_n) \prod_{\substack{i=1 \\ i \neq j}}^n \mu_{v_i \rightarrow a}(x_i) \\
&= \mu_{v_0 \rightarrow a}(0) \left( \sum_{\mathbf{x} \setminus \{x_j\}} (1 - p_2) \prod_{\substack{i=1 \\ i \neq j}}^n \mu_{v_i \rightarrow a}(x_i) + (1 - p_1) \prod_{\substack{i=1 \\ i \neq j}}^n \mu_{v_i \rightarrow a}(1) - (1 - p_2) \prod_{\substack{i=1 \\ i \neq j}}^n \mu_{v_i \rightarrow a}(1) \right) \\
&\quad + \mu_{v_0 \rightarrow a}(1) \left( \sum_{\mathbf{x} \setminus \{x_j\}} p_2 \prod_{\substack{i=1 \\ i \neq j}}^n \mu_{v_i \rightarrow a}(x_i) + p_1 \prod_{\substack{i=1 \\ i \neq j}}^n \mu_{v_i \rightarrow a}(1) - p_2 \prod_{\substack{i=1 \\ i \neq j}}^n \mu_{v_i \rightarrow a}(1) \right) \\
&= \mu_{v_0 \rightarrow a}(0) \left( (1 - p_2) \prod_{\substack{i=1 \\ i \neq j}}^n \sum_{x_i} \mu_{v_i \rightarrow a}(x_i) + (p_2 - p_1) \prod_{\substack{i=1 \\ i \neq j}}^n \mu_{v_i \rightarrow a}(1) \right) \\
&\quad + \mu_{v_0 \rightarrow a}(1) \left( p_2 \prod_{\substack{i=1 \\ i \neq j}}^n \sum_{x_i} \mu_{v_i \rightarrow a}(x_i) + (p_1 - p_2) \prod_{\substack{i=1 \\ i \neq j}}^n \mu_{v_i \rightarrow a}(1) \right) \\
&= ((1 - p_2)\mu_{v_0 \rightarrow a}(0) + p_2\mu_{v_0 \rightarrow a}(1)) \prod_{\substack{i=1 \\ i \neq j}}^n (\mu_{v_i \rightarrow a}(0) + \mu_{v_i \rightarrow a}(1)) \\
&\quad + (p_2 - p_1)(\mu_{v_0 \rightarrow a}(0) - \mu_{v_0 \rightarrow a}(1)) \prod_{\substack{i=1 \\ i \neq j}}^n \mu_{v_i \rightarrow a}(1),
\end{aligned}$$

and

$$\begin{aligned}
\mu_{a \rightarrow v_j}(0) &= \sum_{x_0} \sum_{\mathbf{x} \setminus \{x_j\}} f_a(x_0, \dots, x_{j-1}, 0, x_{j+1}, x_n) \prod_{\substack{i=0 \\ i \neq j}}^n \mu_{v_i \rightarrow a}(x_i) \\
&= \mu_{v_0 \rightarrow a}(0) \sum_{\mathbf{x} \setminus \{x_j\}} f_a(0, \dots, x_{j-1}, 0, x_{j+1}, x_n) \prod_{\substack{i=1 \\ i \neq j}}^n \mu_{v_i \rightarrow a}(x_i) \\
&\quad + \mu_{v_0 \rightarrow a}(1) \sum_{\mathbf{x} \setminus \{x_j\}} f_a(1, \dots, x_{j-1}, 0, x_{j+1}, x_n) \prod_{\substack{i=1 \\ i \neq j}}^n \mu_{v_i \rightarrow a}(x_i) \\
&= \mu_{v_0 \rightarrow a}(0) \sum_{\mathbf{x} \setminus \{x_j\}} (1 - p_2) \prod_{\substack{i=1 \\ i \neq j}}^n \mu_{v_i \rightarrow a}(x_i) + \mu_{v_0 \rightarrow a}(1) \sum_{\mathbf{x} \setminus \{x_j\}} p_2 \prod_{\substack{i=1 \\ i \neq j}}^n \mu_{v_i \rightarrow a}(x_i) \\
&= (1 - p_2)\mu_{v_0 \rightarrow a}(0) \prod_{\substack{i=1 \\ i \neq j}}^n \sum_{x_i} \mu_{v_i \rightarrow a}(x_i) + p_2\mu_{v_0 \rightarrow a}(1) \prod_{\substack{i=1 \\ i \neq j}}^n \sum_{x_i} \mu_{v_i \rightarrow a}(x_i) \\
&= ((1 - p_2)\mu_{v_0 \rightarrow a}(0) + p_2\mu_{v_0 \rightarrow a}(1)) \prod_{\substack{i=1 \\ i \neq j}}^n (\mu_{v_i \rightarrow a}(0) + \mu_{v_i \rightarrow a}(1)).
\end{aligned}$$

For  $v_0$ , we have:

$$\begin{aligned}
\mu_{a \rightarrow v_0}(1) &= \sum_{\mathbf{x}} f_a(1, \mathbf{x}) \prod_{i=1}^n \mu_{v_i \rightarrow a}(x_i) \\
&= \sum_{\mathbf{x}} p_2 \prod_{i=1}^n \mu_{v_i \rightarrow a}(x_i) + p_1 \prod_{i=1}^n \mu_{v_i \rightarrow a}(1) - p_2 \prod_{i=1}^n \mu_{v_i \rightarrow a}(1) \\
&= p_2 \prod_{i=1}^n \sum_{x_i} \mu_{v_i \rightarrow a}(x_i) + (p_1 - p_2) \prod_{i=1}^n \mu_{v_i \rightarrow a}(1) \\
&= p_2 \prod_{i=1}^n (\mu_{v_i \rightarrow a}(0) + \mu_{v_i \rightarrow a}(1)) + (p_1 - p_2) \prod_{i=1}^n \mu_{v_i \rightarrow a}(1).
\end{aligned}$$

Similarly,

$$\mu_{a \rightarrow v_0}(0) = (1 - p_2) \prod_{i=1}^n (\mu_{v_i \rightarrow a}(0) + \mu_{v_i \rightarrow a}(1)) + (p_2 - p_1) \prod_{i=1}^n \mu_{v_i \rightarrow a}(1).$$

The final results are summarized as follows:

$$\begin{aligned}
\mu_{a \rightarrow v_j}(1) &= ((1 - p_2) \mu_{v_0 \rightarrow a}(0) + p_2 \mu_{v_0 \rightarrow a}(1)) \prod_{\substack{i=1 \\ i \neq j}}^n (\mu_{v_i \rightarrow a}(0) + \mu_{v_i \rightarrow a}(1)) \\
&\quad + (p_2 - p_1) (\mu_{v_0 \rightarrow a}(0) - \mu_{v_0 \rightarrow a}(1)) \prod_{\substack{i=1 \\ i \neq j}}^n \mu_{v_i \rightarrow a}(1), \tag{7}
\end{aligned}$$

$$\mu_{a \rightarrow v_j}(0) = ((1 - p_2) \mu_{v_0 \rightarrow a}(0) + p_2 \mu_{v_0 \rightarrow a}(1)) \prod_{\substack{i=1 \\ i \neq j}}^n (\mu_{v_i \rightarrow a}(0) + \mu_{v_i \rightarrow a}(1)), \tag{8}$$

$$\mu_{a \rightarrow v_0}(1) = p_2 \prod_{i=1}^n (\mu_{v_i \rightarrow a}(0) + \mu_{v_i \rightarrow a}(1)) + (p_1 - p_2) \prod_{i=1}^n \mu_{v_i \rightarrow a}(1), \tag{9}$$

$$\mu_{a \rightarrow v_0}(0) = (1 - p_2) \prod_{i=1}^n (\mu_{v_i \rightarrow a}(0) + \mu_{v_i \rightarrow a}(1)) + (p_2 - p_1) \prod_{i=1}^n \mu_{v_i \rightarrow a}(1). \tag{10}$$

For the “OR” factor, from Equation (2) and Table 2b, by following a similar computation process as above, we obtain:

$$\mu_{a \rightarrow v_j}(1) = ((1 - p_1) \mu_{v_0 \rightarrow a}(0) + p_1 \mu_{v_0 \rightarrow a}(1)) \prod_{\substack{i=1 \\ i \neq j}}^n (\mu_{v_i \rightarrow a}(0) + \mu_{v_i \rightarrow a}(1)), \tag{11}$$

$$\begin{aligned}
\mu_{a \rightarrow v_j}(0) &= ((1 - p_1) \mu_{v_0 \rightarrow a}(0) + p_1 \mu_{v_0 \rightarrow a}(1)) \prod_{\substack{i=1 \\ i \neq j}}^n (\mu_{v_i \rightarrow a}(0) + \mu_{v_i \rightarrow a}(1)) \\
&\quad + (p_1 - p_2) (\mu_{v_0 \rightarrow a}(0) - \mu_{v_0 \rightarrow a}(1)) \prod_{\substack{i=1 \\ i \neq j}}^n \mu_{v_i \rightarrow a}(0), \tag{12}
\end{aligned}$$

$$\mu_{a \rightarrow v_0}(1) = p_1 \prod_{i=1}^n (\mu_{v_i \rightarrow a}(0) + \mu_{v_i \rightarrow a}(1)) + (p_2 - p_1) \prod_{i=1}^n \mu_{v_i \rightarrow a}(0), \tag{13}$$

$$\mu_{a \rightarrow v_0}(0) = (1 - p_1) \prod_{i=1}^n (\mu_{v_i \rightarrow a}(0) + \mu_{v_i \rightarrow a}(1)) + (p_1 - p_2) \prod_{i=1}^n \mu_{v_i \rightarrow a}(0). \tag{14}$$

From the above computation formulas, it can be observed that this method exploits the structure of the factor functions to reduce the time complexity of message passing from a factor to a variable—from exponential in the number of neighboring variables to linear. Moreover, the computations above do not alter the messages passed from variables to factors that are dependent on. For simplicity in the following sections, Equation (2) will often be used to denote the dependency relationship, but the actual computations will still be carried out using the formulas derived in this section.

### 3 Motivating Example

We use the factor graph shown in Figure 2b to illustrate the core idea of our approach in this section. To make the approach more accessible, we present a simple factor graph as an example, on which belief propagation converges. However, in practice, factor graphs are almost always loopy and belief propagation may not converge. Figure 2a shows a Bayesian network, assuming that  $P(X_1 = 1) = P(X_2 = 1) = P(X_3 = 1 | (X_1 \wedge X_2) = 1) = p$  and  $P(X_3 = 1 | (X_1 \wedge X_2) = 0) = 0$ . Figure 2b shows the corresponding factor graph transformed from Figure 2a, where  $a_1$ ,  $a_2$ , and  $a_3$  are all “AND” factors, and their factor functions are derived from the (conditional) probabilities.

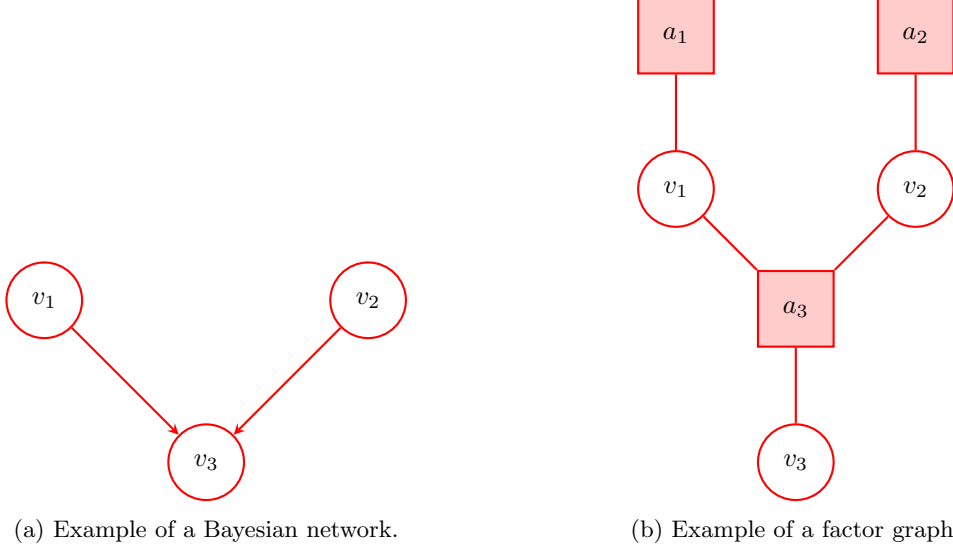


Figure 2: Example of a Bayesian network and the corresponding factor graph. The factor graph is transformed from the Bayesian network.

The first core problem addressed in this paper is how to analyze the message passing dependencies embedded in the computation process of various update strategies. To support diverse update strategies, we represent these dependencies using a strict partially ordered set<sup>4</sup>  $(E, \prec)$  over the edges of the factor graph, which in turn encodes the update strategy. Using  $(E, \prec)$ , we analyze the dependency relationship of a given update strategy and derive a parallel computation process which is equivalent to the original computation given by the strategy. This parallel process partitions the edges into groups and updates the messages of each group in sequence, with messages within each group updated in parallel.

The second core problem is how to perform the message updates within each group in parallel. The key challenge lies in computing messages from factors to variables. As discussed in Section 2.3, Wu et al. [31] modifies the message computation by exploiting the structure of Horn clauses, which prevents us from directly using a single SIMD processor for efficient computation. In this paper, we leverage multiple SIMD processors on a GPU. We further partition the set of factor-to-variable messages into subgroups and compute them using multiple kernel functions<sup>5</sup>.

This section illustrates the core idea of our approach using two update strategies from libDAI [22] as examples. In Subsections 3.1 and 3.2, we first describe the execution process of each strategy in the sequential setting, and then explain how our approach analyzes the dependency relationship embedded in this process to derive an equivalent parallel computation. This section uses concrete examples to demonstrate how our approach operates under different update strategies. A comprehensive framework for systematically analyzing message passing dependencies across various strategies and for parallelizing message updates will be presented in Section 4.

<sup>4</sup>A binary relation  $\prec$  on a set  $A$  is called a strict partial order if it is irreflexive and transitive. The ordered pair  $(A, \prec)$  is then called a strict partially ordered set.

<sup>5</sup>In CUDA (Compute Unified Device Architecture) programming, a kernel function is an extended C++ function. Invoking a kernel launches a set of threads that execute the function in parallel.

### 3.1 Example Update Strategy I: PARALL

The first strategy is called PARALL. In the sequential setting, this strategy updates all factor-to-variable messages once per iteration, in an arbitrary order. When updating a single message from a factor to a variable, the algorithm first computes all required messages from variables to factors. These variable-to-factor messages are derived from the factor-to-variable messages computed in the previous iteration. Using these variable-to-factor messages, the desired factor-to-variable message can then be computed.

In Figure 2b, suppose the messages are updated in the order  $\mu_{a_1 \rightarrow v_1}, \mu_{a_2 \rightarrow v_2}, \mu_{a_3 \rightarrow v_1}, \mu_{a_3 \rightarrow v_2}, \mu_{a_3 \rightarrow v_3}$ . We use superscripts to denote the iteration number. For example,  $\mu^{(i)}$  represents the message at iteration  $i$ , while the absence of a superscript indicates that the message may take multiple values within a single iteration. Consider the  $(i+1)$ -th iteration. According to Equation (2), the update of  $\mu_{a_1 \rightarrow v_1}^{(i+1)}$  does not depend on any variable-to-factor messages and can therefore be computed directly. The same applies to  $\mu_{a_2 \rightarrow v_2}^{(i+1)}$ . Next, the update of  $\mu_{a_3 \rightarrow v_1}^{(i+1)}$  depends on  $\mu_{v_2 \rightarrow a_3}$  and  $\mu_{v_3 \rightarrow a_3}$ . Here,  $\mu_{v_2 \rightarrow a_3}$  is computed using  $\mu_{a_2 \rightarrow v_2}^{(i)}$ , and  $\mu_{v_3 \rightarrow a_3}$  requires no factor-to-variable messages for its computation. Then,  $\mu_{a_3 \rightarrow v_2}^{(i+1)}$  depends on  $\mu_{v_1 \rightarrow a_3}$  and  $\mu_{v_3 \rightarrow a_3}$ , where  $\mu_{v_1 \rightarrow a_3}$  is computed using  $\mu_{a_1 \rightarrow v_1}^{(i)}$ , and again,  $\mu_{v_3 \rightarrow a_3}$  requires no factor-to-variable messages. Finally,  $\mu_{a_3 \rightarrow v_3}^{(i+1)}$  depends on  $\mu_{v_1 \rightarrow a_3}$  and  $\mu_{v_2 \rightarrow a_3}$ , with  $\mu_{v_1 \rightarrow a_3}$  still computed from  $\mu_{a_1 \rightarrow v_1}^{(i)}$  and  $\mu_{v_2 \rightarrow a_3}$  still computed from  $\mu_{a_2 \rightarrow v_2}^{(i)}$ . This completes one full iteration of the computation.

Our approach derives an equivalent parallel computation from the above sequential process. As observed from the computation, within a single iteration, all variable-to-factor messages depend only on factor-to-variable messages from the previous iteration. Therefore, multiple computations of the same variable-to-factor message during one iteration yield identical values. We assign iteration superscripts to variable-to-factor messages as well, and attempt to extend Definition 2.2 to analyze the dependency relationship of message updates:

$$\begin{aligned} \mu_{a \rightarrow v}^{(i+1)}(x_v) &= \sum_{\mathbf{x}_a \setminus x_v} f_a(\mathbf{x}_a) \prod_{v^* \in N_A(a) \setminus \{v\}} \mu_{v^* \rightarrow a}^{(i+1)}(x_{v^*}), \\ \mu_{v \rightarrow a}^{(i+1)}(x_v) &= \prod_{a^* \in N_V(v) \setminus \{a\}} \mu_{a^* \rightarrow v}^{(i)}(x_v). \end{aligned}$$

Within one iteration, updates of factor-to-variable messages are independent. Under this strategy, our approach performs all factor-to-variable message updates in parallel. First, we identify all variable-to-factor messages required by the factor-to-variable messages, which are  $\{\mu_{v_1 \rightarrow a_3}, \mu_{v_2 \rightarrow a_3}, \mu_{v_3 \rightarrow a_3}\}$  in this example. These are computed in parallel using factor-to-variable messages from the previous iteration. Then, using these updated variable-to-factor messages, we simultaneously update all factor-to-variable messages, which are  $\{\mu_{a_1 \rightarrow v_1}, \mu_{a_2 \rightarrow v_2}, \mu_{a_3 \rightarrow v_1}, \mu_{a_3 \rightarrow v_2}, \mu_{a_3 \rightarrow v_3}\}$  in this example.

Figure 3 illustrates the message passing process for one iteration in this example. When updating multiple messages in parallel, we launch one or more kernel functions, with each thread responsible for updating a single message. In the first step, one kernel function is launched to compute the messages using Equation (1). In the second step, two kernel functions are launched. One computes  $\{\mu_{a_3 \rightarrow v_1}, \mu_{a_3 \rightarrow v_2}\}$  using Equations (7)–(8), and the other computes  $\{\mu_{a_1 \rightarrow v_1}, \mu_{a_2 \rightarrow v_2}, \mu_{a_3 \rightarrow v_3}\}$  using Equations (9)–(10). This completes one full iteration of computation in parallel.

### 3.2 Example Update Strategy II: SEQFIX

The second strategy is called SEQFIX. In the sequential setting, this strategy is given a fixed order of factor-to-variable messages, and each iteration updates the messages in this predetermined order. Within an iteration, when updating a message  $\mu_{a \rightarrow v}$  from a factor to a variable, the algorithm first computes all required messages from variables to factors. For such a variable-to-factor message, if it depends on any factor-to-variable message that precedes  $\mu_{a \rightarrow v}$  in the fixed order, values computed in this iteration are used. Otherwise, if it depends on messages that come after  $\mu_{a \rightarrow v}$ , the values from the previous iteration are used.

Again in Figure 2b, suppose the given order is  $\mu_{a_1 \rightarrow v_1}, \mu_{a_2 \rightarrow v_2}, \mu_{a_3 \rightarrow v_1}, \mu_{a_3 \rightarrow v_2}, \mu_{a_3 \rightarrow v_3}$ . Consider the  $(i+1)$ -th iteration. The update of  $\mu_{a_1 \rightarrow v_1}^{(i+1)}$  does not depend on any variable-to-factor messages and can therefore be computed directly. The same applies to  $\mu_{a_2 \rightarrow v_2}^{(i+1)}$ . Next, the update of  $\mu_{a_3 \rightarrow v_1}^{(i+1)}$  depends on  $\mu_{v_2 \rightarrow a_3}$  and  $\mu_{v_3 \rightarrow a_3}$ . Here,  $\mu_{v_2 \rightarrow a_3}$  is computed using  $\mu_{a_2 \rightarrow v_2}^{(i+1)}$ , while  $\mu_{v_3 \rightarrow a_3}$  requires no factor-to-variable messages and can be computed immediately. Then,  $\mu_{a_3 \rightarrow v_2}^{(i+1)}$  depends on  $\mu_{v_1 \rightarrow a_3}$  and  $\mu_{v_3 \rightarrow a_3}$ , where  $\mu_{v_1 \rightarrow a_3}$  is computed using  $\mu_{a_1 \rightarrow v_1}^{(i+1)}$ , and  $\mu_{v_3 \rightarrow a_3}$  is again computed without dependence on any factor-to-variable

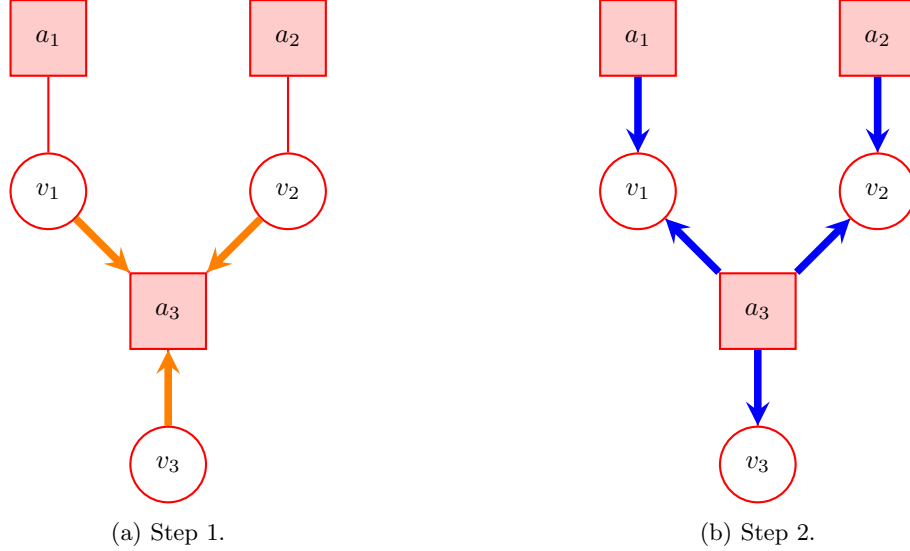


Figure 3: Example of message passing under the PARALL strategy. Bold edges denote message passing. Arrow direction and color denote the message passing direction.

message. Finally,  $\mu_{a_3 \rightarrow v_3}^{(i+1)}$  depends on  $\mu_{v_1 \rightarrow a_3}$  and  $\mu_{v_2 \rightarrow a_3}$ , with  $\mu_{v_1 \rightarrow a_3}$  and  $\mu_{v_2 \rightarrow a_3}$  computed using  $\mu_{a_1 \rightarrow v_1}^{(i+1)}$  and  $\mu_{a_2 \rightarrow v_2}^{(i+1)}$ , respectively. This completes one full iteration of the computation.

Our approach also derives an equivalent parallel computation from the above sequential process. Unlike PARALL, in SEQFIX the update of a factor-to-variable message within an iteration may depend on other messages computed earlier in the same iteration. Therefore, the message updates cannot be simply divided into two global steps. Instead, our approach processes the messages in batches according to the given update order, updating as many messages as possible in parallel at each step. In the above example, the updates of  $\mu_{a_1 \rightarrow v_1}^{(i+1)}$  and  $\mu_{a_2 \rightarrow v_2}^{(i+1)}$  do not require any messages from the current iteration, nor do they depend on any variable-to-factor messages. Hence, they can be updated in parallel in the first batch. However, the update of  $\mu_{a_3 \rightarrow v_1}^{(i+1)}$  depends on  $\mu_{v_2 \rightarrow a_3}$ , which in turn requires  $\mu_{a_2 \rightarrow v_2}^{(i+1)}$  for its computation. Thus,  $\mu_{a_3 \rightarrow v_1}^{(i+1)}$  must wait until  $\mu_{a_2 \rightarrow v_2}^{(i+1)}$  is computed. Therefore, the first batch of messages to be updated in parallel is  $\{\mu_{a_1 \rightarrow v_1}, \mu_{a_2 \rightarrow v_2}\}$ . After this first batch is completed, the remaining three factor-to-variable messages— $\mu_{a_3 \rightarrow v_1}^{(i+1)}$ ,  $\mu_{a_3 \rightarrow v_2}^{(i+1)}$ , and  $\mu_{a_3 \rightarrow v_3}^{(i+1)}$ —depend on a total of three variable-to-factor messages:  $\mu_{v_1 \rightarrow a_3}$ ,  $\mu_{v_2 \rightarrow a_3}$ , and  $\mu_{v_3 \rightarrow a_3}$ . These three messages can now be computed, as they depend only on  $\mu_{a_1 \rightarrow v_1}^{(i+1)}$  and  $\mu_{a_2 \rightarrow v_2}^{(i+1)}$ , both of which are available after the first batch. Once these variable-to-factor messages are computed, the updates of  $\mu_{a_3 \rightarrow v_1}^{(i+1)}$ ,  $\mu_{a_3 \rightarrow v_2}^{(i+1)}$ , and  $\mu_{a_3 \rightarrow v_3}^{(i+1)}$  are independent. Therefore, the second batch to be updated in parallel is  $\{\mu_{a_3 \rightarrow v_1}, \mu_{a_3 \rightarrow v_2}, \mu_{a_3 \rightarrow v_3}\}$ . Before updating the second batch, we first identify the required variable-to-factor messages,  $\{\mu_{v_1 \rightarrow a_3}, \mu_{v_2 \rightarrow a_3}, \mu_{v_3 \rightarrow a_3}\}$ , and compute them in parallel using the results from the first batch in this iteration. Then, the second batch of factor-to-variable messages can be updated in parallel.

Figure 4 illustrates the message-passing process for one iteration in this example under the SEQFIX strategy. In the first step, one kernel function is launched to compute  $\{\mu_{a_1 \rightarrow v_1}, \mu_{a_2 \rightarrow v_2}\}$  using Equations (9)–(10). In the second step, another kernel function is launched to compute the variable-to-factor messages using Equation (1). In the third step, two kernel functions are launched. One computes  $\{\mu_{a_3 \rightarrow v_1}, \mu_{a_3 \rightarrow v_2}\}$  using Equations (7)–(8), and the other computes  $\{\mu_{a_3 \rightarrow v_3}\}$  using Equations (9)–(10). This completes one full iteration of computation in parallel under the SEQFIX strategy.

## 4 Framework

We elaborate on the proposed GPU-accelerated LBP algorithm for program analysis, as well as the FastLBP framework implemented based on the algorithm.

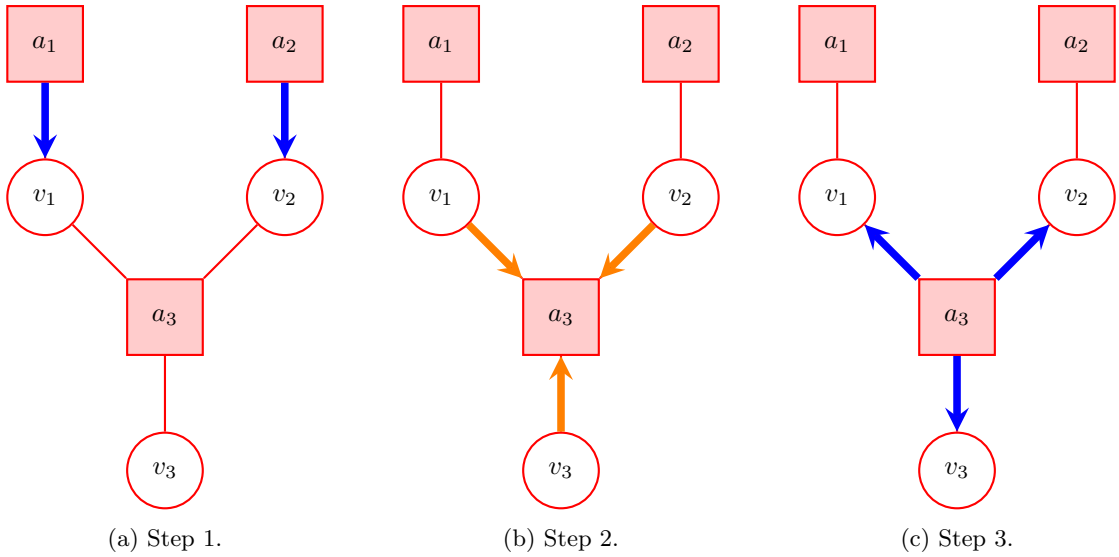


Figure 4: Example of message passing under the SEQFIX strategy. Bold edges denote message passing. Arrow direction and color denote the message passing direction.

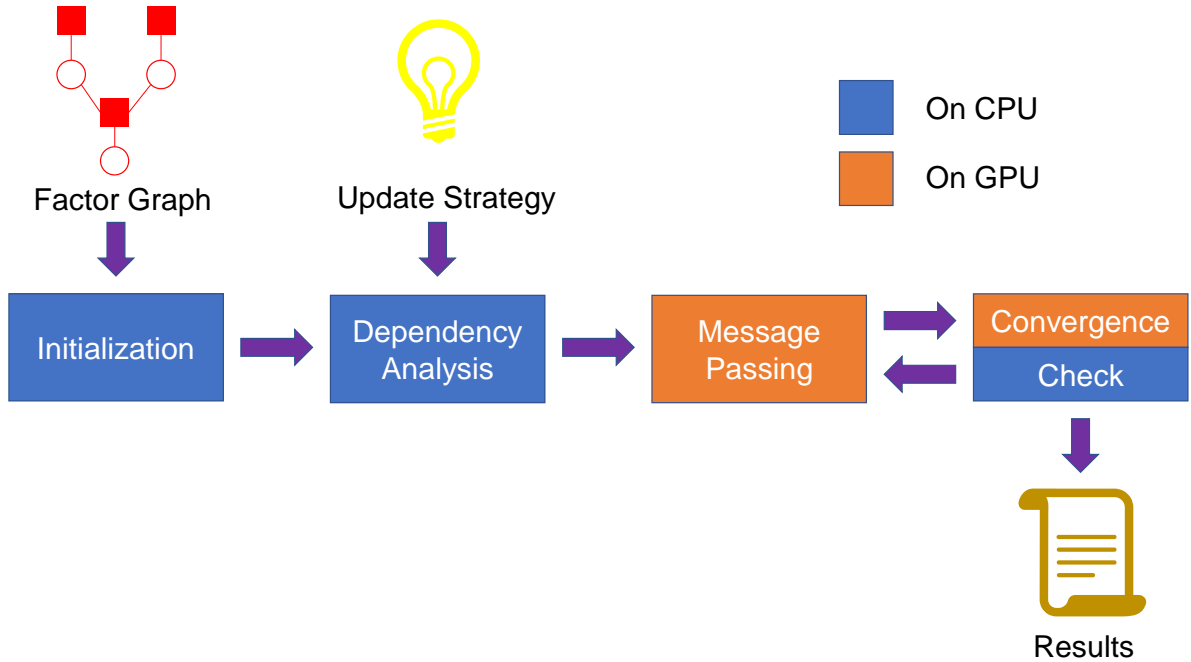


Figure 5: Workflow of the FastLBP framework. Blue components represent operations performed on the CPU, including memory allocation and data transfer between host and device memory. Orange components represent kernel launches and computation on the GPU.

## 4.1 Overview of the FastLBP Framework

Figure 5 illustrates the workflow of the FastLBP framework. The input to FastLBP is a factor graph and an update strategy provided by the user. First, FastLBP takes as input a factor graph that includes all variables, factors, the neighbor relationships for each variable and factor, and the associated factor functions. This factor graph is typically generated through the processes described in Subsection 2.2 and Subsection 2.3. Based on this factor graph, FastLBP allocates memory on the device<sup>6</sup> for storing messages and auxiliary data structures, and performs the corresponding initialization. Next, FastLBP requires the user to specify an update strategy, similar to the motivating examples presented in Section 3. FastLBP represents this update strategy as a strict partially ordered set  $(E, \prec)$  defined over the edges of the factor graph. It then analyzes the dependencies implied by this partially ordered set and partitions the edge set into groups, each representing a set of factor-to-variable messages that can be updated simultaneously. Subsequently, FastLBP identifies the variable-to-factor messages required by each group of factor-to-variable messages. After that, the core message passing phase begins. Message passing proceeds iteratively. In each iteration, messages are updated in the grouping and order determined by the prior dependency analysis. After each iteration, FastLBP performs a convergence check. We compute the marginal probability of each variable using Equation (3). If these probabilities have changed negligibly compared to the previous iteration, the algorithm is considered converged, and the results are output. If not converged, the process returns to the message passing phase for another iteration. Since belief propagation on loopy factor graphs is not guaranteed to converge, we also terminate the computation after a predefined time limit or maximum number of iterations, returning the current iteration’s results as an approximation of the true marginals. Algorithm 1 outlines the overall workflow of the FastLBP framework. The following subsections provide detailed descriptions of the initialization (Line 1), dependency analysis (Lines 2–4), message passing (Lines 7–8), and marginal probability computation (Line 10).

---

### Algorithm 1 Workflow of the FastLBP Framework

---

**Input:** Factor graph  $FG = ((V, A, E), \mathbf{X})$ , update strategy  $ST$   
**Output:** Marginal probabilities  $P(X_1), \dots, P(X_n)$  for all variables

- 1:  $messageVtoF, messageFtoV, auxVtoF, auxFtoV, rowptrFtoV \leftarrow Initialize(FG)$
- 2:  $(E, \prec) \leftarrow GetPoset(FG, ST)$
- 3:  $s_1, \dots, s_k \leftarrow DependencyAnalysis(E, \prec)$  {Each  $s_i$  is a set of edges in the factor graph, representing factor-to-variable messages that can be updated in parallel}
- 4:  $t_1, \dots, t_k \leftarrow GroupVarToFactor(s_1, \dots, s_k)$  {Each  $t_i$  is a set of edges representing variable-to-factor messages that can be updated in parallel}
- 5: **while** not converged **do**
- 6:   **for**  $i \leftarrow 1$  to  $k$  **do**
- 7:      $UpdateMessageVtoF(t_i, messageVtoF, messageFtoV, auxVtoF)$
- 8:      $UpdateMessageFtoV(s_i, messageFtoV, messageVtoF, auxFtoV)$
- 9:   **end for**
- 10:    $P(X_1), \dots, P(X_n) \leftarrow ComputeMarginal(messageFtoV, rowptrFtoV)$
- 11: **end while**
- 12: **return**  $P(X_1), \dots, P(X_n)$

---

## 4.2 Initialization

As a preparatory step for introducing the core algorithm of this paper, this subsection describes how FastLBP performs initialization. A natural and critical question in this phase is: how should data be organized in device memory? On the host side, this question is relatively straightforward. To represent a factor graph, arrays can be used to store the sets of variables and factors, and nested arrays can represent the neighbors of each variable or factor. As stated in Definition 2.2, each edge corresponds to messages in two directions. Such a bipartite graph structure can also be naturally represented using nested array structures. This representation is both convenient and efficient in host memory, where the CPU cache hierarchy helps mitigate memory access latency. However, on the GPU device, using nested arrays leads to frequent global memory accesses, which are expensive in terms of performance.

---

<sup>6</sup>Following CUDA programming terminology, we use host memory to refer to CPU main memory and device memory to refer to GPU memory.

To mitigate this issue, we adopt the approach used in prior work [2, 38], representing all messages and auxiliary data as flat, one-dimensional arrays. This design avoids the use of nested, variable-length arrays and significantly reduces the number of global memory accesses on the GPU. Algorithm 2 describes the initialization procedure. All four main arrays are stored in the Compressed Sparse Row (CSR) format [25], a widely used representation for sparse matrices. Specifically, consider  $messageVtoF$ . We view the variable-to-factor messages as a sparse matrix where each row corresponds to a factor, each column to a variable, and each nonzero entry represents the message from the variable to the factor. If no edge exists between a variable and a factor, the corresponding matrix entry is undefined. By traversing this matrix in row-major order and storing only the nonzero elements sequentially, we obtain the one-dimensional array  $messageVtoF$ . The same CSR layout applies to the other three arrays. The matrix corresponding to  $messageFtoV$  is precisely the transpose of that for  $messageVtoF$ , reflecting the reverse direction of message flow. The auxiliary arrays  $auxVtoF$  and  $auxFtoV$  have the same sparsity pattern as  $messageVtoF$  and  $messageFtoV$ , respectively. They store metadata such as neighbor indices required for efficient message computation at each position. Figure 6 illustrates how messages of the factor graph shown in Figure 2b are stored in device memory using this CSR format.

---

**Algorithm 2** Initialization Function Initialize

---

**Input:** Factor graph  $FG = ((V, A, E), \mathbf{X})$

**Output:** Array  $messageVtoF$  storing variable-to-factor messages,

Array  $messageFtoV$  storing factor-to-variable messages,

Auxiliary data  $auxVtoF$  for computing variable-to-factor messages,

Auxiliary data  $auxFtoV$  for computing factor-to-variable messages,

Index array  $rowptrFtoV$  for marginal probability computation

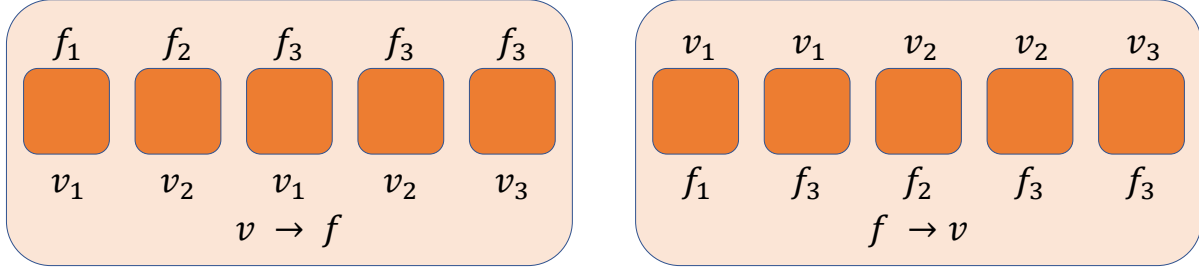
```

1:  $messageVtoF \leftarrow \text{Malloc}(|E| \times \text{sizeof}(message))$ 
2:  $messageFtoV \leftarrow \text{Malloc}(|E| \times \text{sizeof}(message))$ 
3:  $auxVtoF \leftarrow \text{Malloc}(|E| \times \text{sizeof}(aux_1))$ 
4:  $auxFtoV \leftarrow \text{Malloc}(|E| \times \text{sizeof}(aux_2))$  {All four arrays have length  $|E|$ , one entry per directed edge}

5:  $\text{fill}(messageVtoF, 1.0)$ ,  $\text{fill}(messageFtoV, 1.0)$  {Initialize all messages to uniform value 1.0 across all
   variable states}
6:  $rowptrVtoF[0] \leftarrow 0$ ,  $rowptrFtoV[0] \leftarrow 0$ 
7: for  $i \leftarrow 1$  to  $|A|$  do
8:    $rowptrVtoF[i] \leftarrow rowptrVtoF[i - 1] + |N_A(a_i)|$ 
9: end for
10: for  $i \leftarrow 1$  to  $|V|$  do
11:    $rowptrFtoV[i] \leftarrow rowptrFtoV[i - 1] + |N_V(v_i)|$ 
12: end for
13:  $idx \leftarrow 0$ 
14: for  $i \leftarrow 1$  to  $|A|$  do
15:   for  $v$  in  $N_A(a_i)$  do
16:      $startIdx \leftarrow rowptrFtoV[v - 1]$ ,  $endIdx \leftarrow rowptrFtoV[v]$ 
17:      $excludedIdx \leftarrow startIdx + v.\text{dual}$  { $a_i$  is the  $v.\text{dual}$ -th neighbor of  $v$ }
18:      $auxVtoF[idx] \leftarrow \{startIdx, endIdx, excludedIdx\}$ 
19:      $idx \leftarrow idx + 1$ 
20:   end for
21: end for
22:  $idx \leftarrow 0$ 
23: for  $i \leftarrow 1$  to  $|V|$  do
24:   for  $a$  in  $N_V(v_i)$  do
25:      $startIdx \leftarrow rowptrVtoF[a - 1]$ ,  $endIdx \leftarrow rowptrVtoF[a]$ 
26:      $excludedIdx \leftarrow startIdx + a.\text{dual}$  { $v_i$  is the  $a.\text{dual}$ -th neighbor of  $a$ }
27:      $auxFtoV[idx] \leftarrow \{startIdx, endIdx, excludedIdx, a.v0Idx, a.p_1, a.p_2\}$ 
28:      $idx \leftarrow idx + 1$ 
29:   end for
30: end for
31: return  $messageVtoF, messageFtoV, auxVtoF, auxFtoV, rowptrFtoV$ 

```

---



(a) Example of the storage format for messages from variables to factors.

(b) Example of the storage format for messages from factors to variables.

Figure 6: Examples of message storage in device memory.

### 4.3 Dependency Analysis

This subsection provides a detailed exposition of the dependency analysis phase in FastLBP. First, the user provides an update strategy, either one supported natively by FastLBP or a user-defined strategy. FastLBP then formalizes this update strategy as a strict partially ordered set  $(E, \prec)$  over the edge set  $E$  of the factor graph, where  $e_2 \prec e_1$  indicates that the message on edge  $e_2$  must be updated before the message on edge  $e_1$ . Next, FastLBP performs dependency analysis on this strict partially ordered set to partition the edges into ordered groups. The subsequent message passing phase updates messages group by group according to this partitioning, ensuring that the execution respects the user-specified update schedule and produces the intended computational outcome. The remainder of this subsection elaborates on the key components of the dependency analysis algorithm.

**User Interface.** Table 3 illustrates several typical update strategies. The user only needs to specify the strategy name from the left column, and FastLBP uniformly translates it into an intermediate representation, i.e., a strict partially ordered set. Additionally, users may define a custom strict partially ordered set directly as the update strategy.

Table 3: Update Strategies

Strategy Name	Description
PARALL	Update all messages in parallel
SEQFIX	Sequentially update messages in a fixed order
TOPO	Update messages according to topological order for tree-structured factor graphs
...	...

**Intermediate Representation.** To perform dependency analysis for message updates in a uniform manner, we require a unified representation of update dependencies. We observe that common update strategies, in each iteration, update all factor-to-variable messages once. When computing a specific factor-to-variable message, the required variable-to-factor messages must first be computed. These variable-to-factor messages themselves depend on factor-to-variable messages from either the current iteration or the previous iteration. If we treat the computation of variable-to-factor messages as an intermediate step, then the essential dependency lies in whether the required factor-to-variable messages come from the current iteration or the previous iteration. Substituting Equation (1) into Equation (2) and introducing superscripts to denote iteration counts, we obtain:

$$\mu_{a \rightarrow v}^{(i+1)}(x_v) = \sum_{\mathbf{x}_a \setminus x_v} f_a(\mathbf{x}_a) \prod_{v^* \in N_A(a) \setminus \{v\}} \prod_{a^* \in N_V(v^*) \setminus \{a\}} \mu_{a^* \rightarrow v^*}^{(i+\delta((a, v), (a^*, v^*)))}(x_{v^*}), \quad (15)$$

where  $\delta : E \times E \rightarrow \{0, 1\}$ . A valid update strategy must specify a legitimate  $\delta$  function such that the computation remains well-defined and respects the intended scheduling semantics. We now give the definition of intermediate representation used in FastLBP for update strategies, along with the corresponding definitions of  $\delta$ .

**Definition 4.1** (Intermediate Representation of Update Strategies). The intermediate representation of an update strategy is defined as a strict partially ordered set  $(E, \prec)$  on the edge set  $E$  of a factor graph  $FG = ((V, A, E), \mathbf{X})$ . Define the function  $N_E : E \rightarrow \mathcal{P}(E)$  as

$$N_E((a, v)) \stackrel{\text{def}}{=} \bigcup_{v^* \in N_A(a) \setminus \{v\}} \bigcup_{a^* \in N_V(v^*) \setminus \{a\}} \{(a^*, v^*)\}, \quad \forall a \in A, v \in V.$$

Then, given the strict partially ordered set  $(E, \prec)$ , for all  $(a_1, v_1), (a_2, v_2) \in E$ ,

$$\delta((a_1, v_1), (a_2, v_2)) \stackrel{\text{def}}{=} \begin{cases} 1, & \text{if } (a_2, v_2) \prec (a_1, v_1) \text{ and } (a_2, v_2) \in N_E((a_1, v_1)), \\ 0, & \text{otherwise.} \end{cases}$$

The message update is performed according to Equation (15).

The following Theorem 4.1 shows that the function  $\delta$  defined in Definition 4.1 is legitimate.

**Theorem 4.1** (Legality of Update Strategy Representation). If the function  $\delta$  is given by Definition 4.1, then there does not exist a sequence of edges  $e_{j_1}, e_{j_2}, \dots, e_{j_p} \in E$  (with  $p > 1$ ) such that

$$e_{j_1} = e_{j_p} \quad \text{and} \quad \forall 1 \leq i < p, \delta(e_{j_i}, e_{j_{i+1}}) = 1.$$

*Proof.* We proceed by contradiction. Suppose such a sequence exists.

When  $p = 2$ , we have  $e_{j_1} = e_{j_2}$  and  $\delta(e_{j_1}, e_{j_2}) = 1$ . However, by Definition 4.1,  $\delta(e_{j_1}, e_{j_2}) = 1$  implies  $e_{j_2} \prec e_{j_1}$ . Since  $e_{j_1} = e_{j_2}$ , this implies  $e_{j_1} \prec e_{j_1}$ , which contradicts the irreflexivity of the strict partial order  $\prec$ .

For  $p > 2$ , by Definition 4.1,  $\delta(e_{j_i}, e_{j_{i+1}}) = 1$  for all  $1 \leq i < p$  implies  $e_{j_i} \prec e_{j_{i+1}}$ . Thus, by transitivity of  $\prec$ , it follows that  $e_{j_1} \prec e_{j_p}$ . But since  $e_{j_1} = e_{j_p}$ , this yields  $e_{j_1} \prec e_{j_1}$ , again contradicting the irreflexivity of  $\prec$ .

Therefore, no such cyclic sequence can exist, completing the proof.  $\square$

Theorem 4.1 shows that the update strategy defined by Definition 4.1 contains no cyclic dependencies. That is, within a single iteration, starting from any message, although it may depend on other messages computed in the current iteration, and those messages in turn may depend on yet others from the same iteration, this chain of dependencies must eventually terminate at messages whose values are taken from the previous iteration. This termination is guaranteed by the finiteness of the edge set  $E$ . Therefore, the current iteration's results can always be computed starting from the messages of the previous iteration, which confirms the well-definedness and correctness of Definition 4.1. Intuitively, specifying that  $e_1 \prec e_2$  in the strict partial order means that, during one iteration, the message on edge  $e_2$  must use the current-iteration value of the message on edge  $e_1$ . Definition 4.1 captures a sufficiently broad subset of valid update strategies. For example, PARALL is represented by the empty relation, SEQFIX corresponds to a total order over all edges, and TOPO is expressed as a topological order.

**Dependency Analysis Algorithm.** We now present the dependency analysis algorithm based on the intermediate representation of the update strategy.

In Algorithm 3, TopologicalSort on line 1 refers to a topological sorting performed on the Hasse diagram<sup>7</sup> of the strict partially ordered set. To enhance concurrency, the topological sort may traverse the graph in a breadth-first manner. After the topological sorting, the algorithm greedily groups edges into batches. When processing edge  $e_i$ , if it depends on any edge already in  $NextSet$ , then the current  $NextSet$  is output as a batch, and a new batch  $\{e_i\}$  is started. Finally, the algorithm outputs a sequence of edge sets. Updating factor-to-variable messages in the order of this sequence yields the expected result under the specified update strategy. Theorem 4.2 establishes the correctness of this algorithm, guaranteeing that when updating messages in a given batch, all required dependencies have already been computed in previous batches or are available from the previous iteration.

**Theorem 4.2** (Correctness of the Dependency Analysis Algorithm). For all  $s_j \in \{s_1, \dots, s_k\}$ , for all  $e = (a, v) \in E$ , and for all  $e' \in N_E(e)$ , if  $e' \prec e$ , then  $e' \in \bigcup_{1 \leq l < j} s_l$ .

*Proof.* Since  $e' \prec e$ , by line 1,  $e' \in \bigcup_{1 \leq l \leq j} s_l$ . Moreover, because  $e' \in N_E(e)$  and  $e' \prec e$ , lines 5–9 ensure that  $e' \notin s_j$ . Combining both facts, we conclude that  $e' \in \bigcup_{1 \leq l < j} s_l$ .  $\square$

<sup>7</sup>The Hasse diagram can be represented as a directed acyclic graph (DAG), where each element of the set corresponds to a node. There is a directed edge from node  $e'$  to node  $e''$  if  $e' \prec e''$  and there does not exist an element  $e'''$  such that  $e' \prec e'''$  and  $e''' \prec e''$ .

---

**Algorithm 3** Dependency Analysis Algorithm: DependenceAnalysis

---

**Input:** A strict partially ordered set  $(E, \prec)$ , where  $E = \{e_1, \dots, e_N\}$

**Output:** A sequence of edge sets  $s_1, \dots, s_k$

```
1:  $e_1, \dots, e_N \leftarrow \text{TopologicalSort}(E, \prec)$ 
2:  $NextSet \leftarrow \emptyset$ 
3: for  $i \leftarrow 1$  to  $N$  do
4:   for  $e$  in  $NextSet$  do
5:     if  $e \in N_E(e_i)$  and  $e \prec e_i$  then
6:       Output  $NextSet$ 
7:        $NextSet \leftarrow \{e_i\}$ 
8:       goto 3
9:     end if
10:   end for
11: end for
12: Output  $NextSet$ 
```

---

Before computing factor-to-variable messages, the corresponding variable-to-factor messages must first be computed. The following algorithm computes, from a given set of factor-to-variable edges, the set of variable-to-factor edges they depend on. It is worth noting that, according to Definition 4.1, a single edge may correspond to multiple variable-to-factor messages. In such cases, this paper relaxes the requirement on the function  $\delta$ . When  $(a_2, v_2) \not\prec (a_1, v_1)$  but  $e_2 \in N_E(e_1)$ , either  $\delta((a_1, v_1), (a_2, v_2)) = 0$  or 1 is acceptable. Since  $\delta$  is defined within a computational context, cyclic dependencies remain impossible even under this relaxation.

---

**Algorithm 4** Function GROUPVARTOFACTOR

---

**Input:** A sequence of edge sets  $s_1, \dots, s_k$

**Output:** A sequence of edge sets  $t_1, \dots, t_k$ , corresponding to the input sets

```
1: for  $i \leftarrow 1$  to  $k$  do
2:    $t_i \leftarrow \emptyset$ 
3:   for  $(a, v)$  in  $s_i$  do
4:      $t_i \leftarrow t_i \cup \{(v^*, a) \mid v^* \in N_A(a) \setminus \{v\}\}$ 
5:   end for
6: end for
7: return  $t_1, \dots, t_k$ 
```

---

## 4.4 Message Passing

So far, we have established the message storage arrays, auxiliary data structures for message computation, and groups of messages that can be updated in parallel. In this subsection, we address the second core problem of this paper: how to perform message passing in parallel.

The first step of message passing is to compute the variable-to-factor messages according to Equation (1). Algorithm 5 presents the detailed computation procedure. Each thread computes the message on one edge, and all messages within a group are computed independently and in parallel.

The second step of message passing is to compute the factor-to-variable messages according to Equations (7)–(14). Unlike variable-to-factor messages, factor-to-variable messages cannot be computed using a single uniform formula. This leads to the challenge of designing efficient kernel functions for their parallel computation. One possible approach is to pass the message computation type as a parameter to a unified kernel, and use conditional branching to select the appropriate formula. However, in GPU programming, conditional statements should be avoided whenever possible, as they can cause severe warp divergence. Specifically, when a kernel executes a branch, if only a subset of threads within a warp take one path, the remaining threads must idle until that path completes. To minimize warp divergence, this paper assigns a separate kernel function to each message computation pattern. Furthermore, we observe significant computational overlap across different message values on the same edge. For example, Equations (7) and (8) both include the common subexpression  $((1 - p_2)\mu_{v_0 \rightarrow a}(0) + p_2\mu_{v_0 \rightarrow a}(1)) \prod_{\substack{i=1 \\ i \neq j}}^n (\mu_{v_i \rightarrow a}(0) + \mu_{v_i \rightarrow a}(1))$ . This term can be computed once and reused, reducing both memory accesses and arithmetic operations.

---

**Algorithm 5 Kernel Function UPDATERMESSAGEVTOF**

---

**Input:** A set of edges  $t$  (converted to corresponding indices in arrays  $messageVtoF$  and  $auxVtoF$ ),  
array  $messageVtoF$  storing variable-to-factor messages,  
array  $messageFtoV$  storing factor-to-variable messages,  
auxiliary data  $auxVtoF$  required for computing variable-to-factor messages

**Output:** Updated variable-to-factor messages stored in  $messageVtoF$

```
1:  $threadId \leftarrow blockIdx.x \times blockDim.x + threadIdx.x$  {Get global thread index}
2:  $messageIdx \leftarrow t[threadId]$  {Get index of the message to update}
3:  $startIdx, endIdx, excludedIdx \leftarrow auxVtoF[messageIdx]$ 
4:  $message \leftarrow 1.0$ 
5: for  $i \leftarrow startIdx$  to  $endIdx$  do
6:   if  $i \neq excludedIdx$  then
7:      $message \leftarrow message \times messageFtoV[i]$ 
8:   end if
9: end for
10:  $messageVtoF[messageIdx] \leftarrow message$ 
```

---

Therefore, we implement four specialized kernel functions, each handling a pair of related message types, one kernel for Equations (7) and (8), one for Equations (9) and (10), one for Equations (11) and (12), and one for Equations (13) and (14). Algorithms 6–10 present the overall workflow and the four kernel implementations, respectively.

---

**Algorithm 6 Function UPDATERMESSAGEFTOV**

---

**Input:** A set of edges  $s$  (converted to corresponding indices in arrays  $messageFtoV$  and  $auxFtoV$ ),  
array  $messageFtoV$  storing factor-to-variable messages,  
array  $messageVtoF$  storing variable-to-factor messages,  
auxiliary data  $auxFtoV$  required for computing factor-to-variable messages

**Output:** Updated factor-to-variable messages stored in  $messageFtoV$

```
1:  $es_1, es_2, es_3, es_4 \leftarrow \text{split}(s)$  {Partition  $s$  into four subsets; messages on edges in each subset are computed by one of the four kernel functions}
2:  $\text{UpdateMessageFtoVand1}(es_1, messageFtoV, messageVtoF, auxFtoV)$ 
3:  $\text{UpdateMessageFtoVand2}(es_2, messageFtoV, messageVtoF, auxFtoV)$ 
4:  $\text{UpdateMessageFtoVor1}(es_3, messageFtoV, messageVtoF, auxFtoV)$ 
5:  $\text{UpdateMessageFtoVor2}(es_4, messageFtoV, messageVtoF, auxFtoV)$ 
```

---

## 4.5 Marginal Probability Computation

Finally, this subsection describes how to compute variable marginal probabilities in parallel. According to Equation (3), we assign one thread per variable to compute the product of incoming factor-to-variable messages, followed by normalization. Algorithm 11 outlines the procedure for marginal probability computation. Once the marginal probabilities are obtained, convergence can be checked using methods from prior work [22].

## 5 Evaluation

This section presents two experiments designed to evaluate the efficiency and accuracy of FastLBP. We aim to answer the following research questions:

- **RQ1.** How accurate is FastLBP compared to state-of-the-art serial methods?
- **RQ2.** How fast is FastLBP compared to state-of-the-art serial methods?
- **RQ3.** How accurate is FastLBP compared to state-of-the-art GPU-based parallel methods?
- **RQ4.** How fast is FastLBP compared to state-of-the-art GPU-based parallel methods?

---

**Algorithm 7 Kernel Function UPDATEMESSAGEFTOVAND1**

---

**Input:**  $es, messageFtoV, messageVtoF, auxFtoV$   
**Output:** Updated factor-to-variable messages stored in  $messageFtoV$

```
1:  $threadId \leftarrow blockIdx.x \times blockDim.x + threadIdx.x$  {Get global thread index}
2:  $messageIdx \leftarrow es[threadId]$  {Get index of the message to update}
3:  $startIdx, endIdx, excludedIdx, v0Idx, p1, p2 \leftarrow auxFtoV[messageIdx]$ 
4:  $prod_1 \leftarrow 1.0, prod_2 \leftarrow p_2 - p_1$ 
5: for  $i \leftarrow startIdx$  to  $endIdx$  do
6:   if  $i = v0Idx$  then
7:      $prod_1 \leftarrow prod_1 \times ((1 - p_2) \times messageVtoF[i][0] + p_2 \times messageVtoF[i][1])$ 
8:      $prod_2 \leftarrow prod_2 \times (messageVtoF[i][0] - messageVtoF[i][1])$ 
9:   else if  $i \neq excludedIdx$  then
10:     $prod_1 \leftarrow prod_1 \times (messageVtoF[i][0] + messageVtoF[i][1])$ 
11:     $prod_2 \leftarrow prod_2 \times messageVtoF[i][1]$ 
12:   end if
13: end for
14:  $messageFtoV[messageIdx][1] \leftarrow prod_1 + prod_2$ 
15:  $messageFtoV[messageIdx][0] \leftarrow prod_1$ 
```

---

---

**Algorithm 8 Kernel Function UPDATEMESSAGEFTOVAND2**

---

**Input:**  $es, messageFtoV, messageVtoF, auxFtoV$   
**Output:** Updated factor-to-variable messages stored in  $messageFtoV$

```
1:  $threadId \leftarrow blockIdx.x \times blockDim.x + threadIdx.x$  {Get global thread index}
2:  $messageIdx \leftarrow es[threadId]$  {Get index of the message to update}
3:  $startIdx, endIdx, excludedIdx, v0Idx, p1, p2 \leftarrow auxFtoV[messageIdx]$ 
4:  $prod_1 \leftarrow 1.0, prod_2 \leftarrow p_2 - p_1$ 
5: for  $i \leftarrow startIdx$  to  $endIdx$  do
6:   if  $i \neq excludedIdx$  then
7:      $prod_1 \leftarrow prod_1 \times (messageVtoF[i][0] + messageVtoF[i][1])$ 
8:      $prod_2 \leftarrow prod_2 \times messageVtoF[i][1]$ 
9:   end if
10: end for
11:  $messageFtoV[messageIdx][1] \leftarrow p_2 \times prod_1 - prod_2$ 
12:  $messageFtoV[messageIdx][0] \leftarrow (1 - p_2) \times prod_1 + prod_2$ 
```

---

---

**Algorithm 9 Kernel Function UPDATEMESSAGEFTOVOR1**

---

**Input:**  $es, messageFtoV, messageVtoF, auxFtoV$   
**Output:** Updated factor-to-variable messages stored in  $messageFtoV$

```
1:  $threadId \leftarrow blockIdx.x \times blockDim.x + threadIdx.x$  {Get global thread index}
2:  $messageIdx \leftarrow es[threadId]$  {Get index of the message to update}
3:  $startIdx, endIdx, excludedIdx, v0Idx, p1, p2 \leftarrow auxFtoV[messageIdx]$ 
4:  $prod_1 \leftarrow 1.0, prod_2 \leftarrow p_2 - p_1$ 
5: for  $i \leftarrow startIdx$  to  $endIdx$  do
6:   if  $i = v0Idx$  then
7:      $prod_1 \leftarrow prod_1 \times ((1 - p_1) \times messageVtoF[i][0] + p_1 \times messageVtoF[i][1])$ 
8:      $prod_2 \leftarrow prod_2 \times (messageVtoF[i][0] - messageVtoF[i][1])$ 
9:   else if  $i \neq excludedIdx$  then
10:     $prod_1 \leftarrow prod_1 \times (messageVtoF[i][0] + messageVtoF[i][1])$ 
11:     $prod_2 \leftarrow prod_2 \times messageVtoF[i][0]$ 
12:   end if
13: end for
14:  $messageFtoV[messageIdx][1] \leftarrow prod_1$ 
15:  $messageFtoV[messageIdx][0] \leftarrow prod_1 + prod_2$ 
```

---

---

**Algorithm 10 Kernel Function UPDATEMESSAGEFTOVOR2**

---

**Input:**  $es, messageFtoV, messageVtoF, auxFtoV$   
**Output:** Updated factor-to-variable messages stored in  $messageFtoV$

```
1:  $threadId \leftarrow blockIdx.x \times blockDim.x + threadIdx.x$  {Get global thread index}
2:  $messageIdx \leftarrow es[threadId]$  {Get index of the message to update}
3:  $startIdx, endIdx, excludedIdx, v0Idx, p1, p2 \leftarrow auxFtoV[messageIdx]$ 
4:  $prod_1 \leftarrow 1.0, prod_2 \leftarrow p_2 - p_1$ 
5: for  $i \leftarrow startIdx$  to  $endIdx$  do
6:   if  $i \neq excludedIdx$  then
7:      $prod_1 \leftarrow prod_1 \times (messageVtoF[i][0] + messageVtoF[i][1])$ 
8:      $prod_2 \leftarrow prod_2 \times messageVtoF[i][0]$ 
9:   end if
10: end for
11:  $messageFtoV[messageIdx][1] \leftarrow p_1 \times prod_1 + prod_2$ 
12:  $messageFtoV[messageIdx][0] \leftarrow (1 - p_2) \times prod_1 - prod_2$ 
```

---

**Algorithm 11 Kernel Function COMPUTEMARGINAL**

---

**Input:** Array  $messageFtoV$  storing factor-to-variable messages,  
index array  $rowptrFtoV$  indicating the start and end positions of messages for each variable  
**Output:** Marginal probabilities  $P(X_1), \dots, P(X_n)$

```
1:  $threadId \leftarrow blockIdx.x \times blockDim.x + threadIdx.x$  {Get global thread index}
2:  $prod_0 \leftarrow 1.0, prod_1 \leftarrow 1.0$ 
3: for  $i \leftarrow rowptrFtoV[threadId]$  to  $rowptrFtoV[threadId + 1]$  do
4:    $prod_0 \leftarrow prod_0 \times messageFtoV[i][0]$ 
5:    $prod_1 \leftarrow prod_1 \times messageFtoV[i][1]$ 
6: end for
7:  $P(X_{threadId} = 0) \leftarrow prod_0 / (prod_0 + prod_1)$ 
8:  $P(X_{threadId} = 1) \leftarrow 1 - P(X_{threadId} = 0)$ 
```

---

## 5.1 Experimental Setup

FastLBP is implemented in C++/CUDA. The implementation for reading factor graphs and storing them in host memory is based on libDAI [22] and its extension [7]. The frontend provides a user interface compatible with libDAI. All experiments in this paper are conducted within the BINGO framework [27]. BINGO is built upon the Bayesian program analysis introduced in Section 2. We compare the performance of different approaches in running LBP for Bayesian inference within the BINGO framework. All experiments are conducted on a Linux machine with a 2.10 GHz processor and 251 GiB memory, using an NVIDIA RTX 2080 Ti GPU with 11 GiB memory.

### 5.1.1 Program Analysis

The experiments in this paper use the same datarace analysis as in [27]. We perform Datalog program analysis using the Chord framework [24] for Java programs. The datarace analysis combines flow-sensitive and context-sensitive thread-escape, may-happen-in-parallel, and lockset analysis. These analyses are built upon a call graph and aliasing information derived from a 3-context-and-object-sensitive, but flow-insensitive pointer analysis [21].

### 5.1.2 Benchmarks

We use the same set of 8 benchmark programs as in [27], which have also been widely adopted in prior work [3, 10, 36, 37]. The characteristics of the benchmarks are summarized in Table 4. After performing datarace analysis on these benchmarks and reducing the resulting graphs using the BINGO framework, the numbers of tuples, clauses, and reported alarms are shown in Table 5. Note that the sum of the number of tuples and clauses equals the number of vertices in the corresponding Bayesian network (see Table 1).

Table 4: Benchmark characteristics. ‘‘Total’’ and ‘‘App’’ are numbers with and without the JDK using 0-CFA call graph construction

Program	Description	# Classes		# Methods		Bytecode (KB)		Source (KLOC)	
		App	Total	App	Total	App	Total	App	Total
weblech	Website download/mirror tool	56	1,276	303	8,421	18	503	10	322
hedc	Web crawler from ETH	44	1,157	230	7,501	15	464	6	292
luindex	Document indexing tool	169	1,164	1,030	7,461	72	453	30	299
jspider	Web spider engine	113	1,193	426	7,431	17	429	6.7	298
avrora	AVR microcontroller simulator	1,119	2,080	3,875	10,095	191	553	54	318
xalan	XML to HTML transforming tool	390	1,723	3,007	12,181	159	786	119	495
sunflow	Photo-realistic image rendering system	127	1,853	967	12,901	87	878	15	529
ftp	Apache FTP server	119	1,196	608	7,650	35	443	17	305

Table 5: Number of tuples, clauses, and alarms.

Program	# Tuples	# Clauses	# Alarms		
			True	False	Total
weblech	313	383	6	24	30
hedc	2,223	3,124	12	130	152
luindex	5,334	6,523	2	938	940
jspider	9,501	15,661	9	248	257
avrora	12,411	23,680	29	949	978
xalan	19,011	32,809	75	1,795	1,870
sunflow	59,722	96,973	171	787	958
ftp	98,093	113,082	75	447	522

### 5.1.3 Baselines

We compare FastLBP against two baselines: Wu et al. [31] and PGMax [38]. Chen et al. extended the libDAI library [22] and implemented the method of Wu et al. in the library [7]. In this paper, we use this extended library [7] as the implementation of the state-of-the-art sequential method. libDAI [22] is a free and open-source C++ library that provides a wide range of inference algorithms for discrete probabilistic graphical models, including LBP. It supports various message update strategies. The work by [27] also employs libDAI for Bayesian inference. PGMax [38] is a Python/JAX [4] package that implements LBP for discrete probabilistic graphical models. It only supports the fully parallel (PARALL) update strategy with a fixed number of iterations. Supporting other update strategies would incur significant performance degradation. However, since JAX supports GPU acceleration, PGMax can run on GPUs. To the best of our knowledge, PGMax is the only GPU-accelerated method that supports arbitrary-shaped probabilistic graphical models. Other existing GPU-based approaches are restricted to specific graph structures and are therefore not applicable to our use case in program analysis. Hence, we adopt PGMax as the state-of-the-art GPU-based parallel baseline in our evaluation.

### 5.1.4 Evaluation Metrics

We use three metrics to evaluate the accuracy of marginal probabilities computed by LBP, and two metrics to evaluate its runtime performance. In the BINGO framework, the user interactively selects the alarm with the highest predicted true probability for labeling in each round. Let  $l_1, \dots, l_n \in \{0, 1\}$  denote the ground-truth labels of the alarms provided by the user, and let  $t_1, \dots, t_n$  denote the runtime of each interaction round.

**Rank-100%-T: Number of interactions to identify 100% of true alarms.** This metric measures how many alarms the user are required to label before all true alarms are discovered. The more accurate the LBP results, the better the ranking of alarms, and the sooner the user can find all true positives. Formally,

$$\text{Rank-100%-T} = \min \left\{ i \mid \sum_{j=1}^i l_j = \sum_{j=1}^n l_j \right\}.$$

**Rank-90%-T: Number of interactions to identify 90% of true alarms.** This metric measures the number of user interactions required to discover the majority of true alarms. Since some alarms have weak dependencies and may be discovered late, this metric mitigates the impact of extreme cases. Formally,

$$\text{Rank-90%-T} = \min \left\{ i \mid 10 \sum_{j=1}^i l_j \geq 9 \sum_{j=1}^n l_j \right\}.$$

**Inversion: Number of inversions in the ranking.** An inversion occurs when a false alarm is ranked higher than a true alarm in the user’s labeling sequence. This metric evaluates the quality of the alarm ranking, thereby reflecting the accuracy of LBP in this task. Formally,

$$\text{Inversion} = \sum_{i=1}^n (1 - l_i) \sum_{j=i+1}^n l_j.$$

**TotalTime: Total execution time.** This is the cumulative runtime of the BINGO framework until all true alarms are identified. Formally,

$$\text{TotalTime} = \sum_{i=1}^{\text{Rank-100%-T}} t_i.$$

**AverageTime: Average per-round execution time.** This is the average time per interaction round over the entire process of identifying all true alarms. Formally,

$$\text{AverageTime} = \frac{\text{TotalTime}}{\text{Rank-100%-T}}.$$

## 5.2 Experiment 1: Comparison with Sequential Method (RQ1 and RQ2)

To answer RQ1 and RQ2, we compare FastLBP against the method of Wu et al. [31] running in single-threaded mode. In Bayesian program analysis, the SEQFIX update strategy is commonly used to achieve better convergence and accuracy. Therefore, this experiment adopts SEQFIX as the update strategy for both methods. The maximum number of iterations is set to 1000.

**Accuracy.** Table 6 summarizes the results of the three accuracy metrics. Compared to the method of Wu et al., FastLBP shows average relative changes of  $-7.34\%$ ,  $+1.65\%$ , and  $+4.40\%$  in Rank-100%-T, Rank-90%-T, and Inversion, respectively. This indicates that the results produced by FastLBP are highly accurate and nearly indistinguishable from those of the sequential method. Theoretically, FastLBP should produce identical results to the sequential implementation under the same update strategy. The small discrepancies observed in practice are primarily due to differences in numerical error accumulation between the two implementations. In general, larger numerical errors lead to worse inference quality. Prior implementations [22, 7] employ various techniques to mitigate numerical instability and achieve higher precision. The results demonstrate that FastLBP has effective control over numerical errors.

To illustrate the dynamic process of identifying true and false alarms, we plot ROC curves [11] in Figure 7. In these curves, the horizontal and vertical axes represent the cumulative number of false and true alarms identified so far, respectively. A point  $(x, y)$  on the curve indicates that after  $x + y$  interaction rounds,  $x$  false alarms and  $y$  true alarms have been discovered. The normalized area under the ROC curve (AUC) serves as another accuracy metric. AUC is directly related to the number of inversions  $\text{Inversion} = N_T N_F (1 - \text{AUC})$ , where  $N_T$  is the total number of true alarms and  $N_F$  is the total number of false alarms. As shown in Figure 7, the ROC curves of FastLBP and Wu et al. are either perfectly overlapping or nearly identical across most benchmarks. The AUC values are also very close. Only on the avrora benchmark does FastLBP exhibit a noticeably lower AUC.

In summary, the parallel approach of FastLBP achieves almost identical accuracy compared to its sequential counterpart. The marginal probabilities produced by the LBP using FastLBP have negligible impact on the user interaction experience.

**Execution Speed.** Figure 8 shows the number of true alarms identified over time by Wu et al. and FastLBP, respectively. On most benchmarks, FastLBP identifies all true alarms in significantly less time. The two exceptions are weblech and hedc, where the Bayesian networks are relatively small (see Tables 1

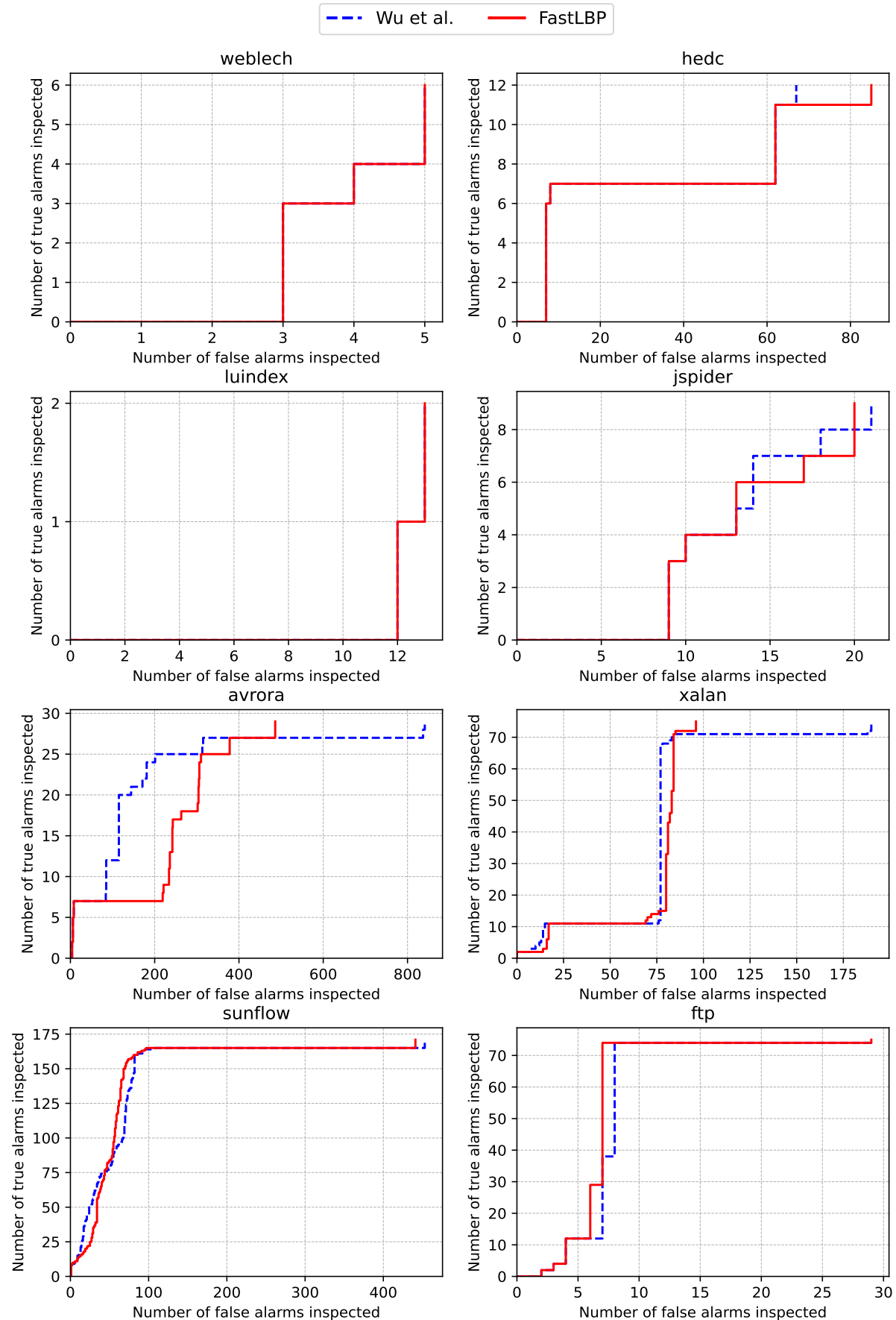


Figure 7: Comparison of ROC curves between Wu et al. and FastLBP.

Table 6: Accuracy for Wu et al. and FastLBP. The average relative change is the arithmetic mean of individual relative changes.

Program	Rank-100%-T		Rank-90%-T		Inversion	
	Wu et al.	FastLBP	Wu et al.	FastLBP	Wu et al.	FastLBP
weblech	11	11	11	11	23	23
hedc	79	97	73	73	365	383
luindex	15	15	15	15	25	25
jspider	30	29	30	29	117	120
avrora	870	515	342	405	4,570	6,519
xalan	265	171	146	152	5,510	5,396
sunflow	624	612	236	225	10,565	10,238
ftp	104	104	76	75	541	488
Average Relative Change	7.34% ↓		1.65% ↑		4.40% ↑	

and 5). Under the constraints of the SEQFIX update strategy, FastLBP cannot achieve high parallelism on these small graphs, and the performance gain from GPU-based parallel computation fails to offset the overhead introduced by dependency analysis and memory transfers. As the graph size increases, the advantage of FastLBP becomes increasingly evident. On luindex and jspider, FastLBP is slightly faster than Wu et al.. On the four benchmarks avrora, xalan, sunflow, and ftp, FastLBP runs several times faster. Although FastLBP is marginally slower on small-scale graphs, this has negligible practical impact because the total time required for LBP on such graphs is inherently small, which is less than 15 minutes on weblech, hedc, luindex, and jspider to identify all true alarms. Thus, the performance difference does not significantly affect user experience. In contrast, users are primarily concerned with execution time on large-scale graphs, where total runtime can extend to several hours or even exceed one day, as observed in avrora, xalan, sunflow, and ftp. It is precisely in these large-scale scenarios that FastLBP excels, significantly accelerating LBP and substantially reducing user waiting time.

Table 7 presents detailed data on total execution time and average execution time. Compared to Wu et al., FastLBP achieves speedups of  $2.14\times$  in total execution time and  $1.93\times$  in average execution time. When excluding benchmarks where Wu et al. takes less than 15 minutes in total (i.e., `weblech`, `hedc`, `luindex`, and `jspider`), the speedups increase to  $5.60\times$  and  $4.38\times$ , respectively. In summary, FastLBP significantly accelerates LBP compared to the state-of-the-art sequential method, especially on large-scale probabilistic graphical models.

Table 7: Execution time for Wu et al. and FastLBP. The average speedup is the geometric mean of individual speedups.

Benchmark	TotalTime (s)		AverageTime (s)	
	Wu et al.	FastLBP	Wu et al.	FastLBP
weblech	2.87	7.66	0.26	0.70
hedc	277.15	414.32	3.51	4.27
luindex	90.68	71.83	6.05	4.79
jspider	890.31	629.84	29.68	21.72
avrora	43139.65	7038.20	49.59	13.67
xalan	16620.20	3801.29	62.72	22.23
sunflow	89968.12	20661.15	144.18	33.76
ftp	28816.21	3426.42	277.08	32.95
Average Speedup	$2.14\times$		$1.93\times$	

### 5.3 Experiment 2: Comparison with GPU-Based Parallel Method (RQ3 and RQ4)

To answer RQ3 and RQ4, we compare our approach with PGMax [38], using the NVIDIA GPU version of JAX for this experiment. Since PGMax supports only the PARALL update strategy and requires a

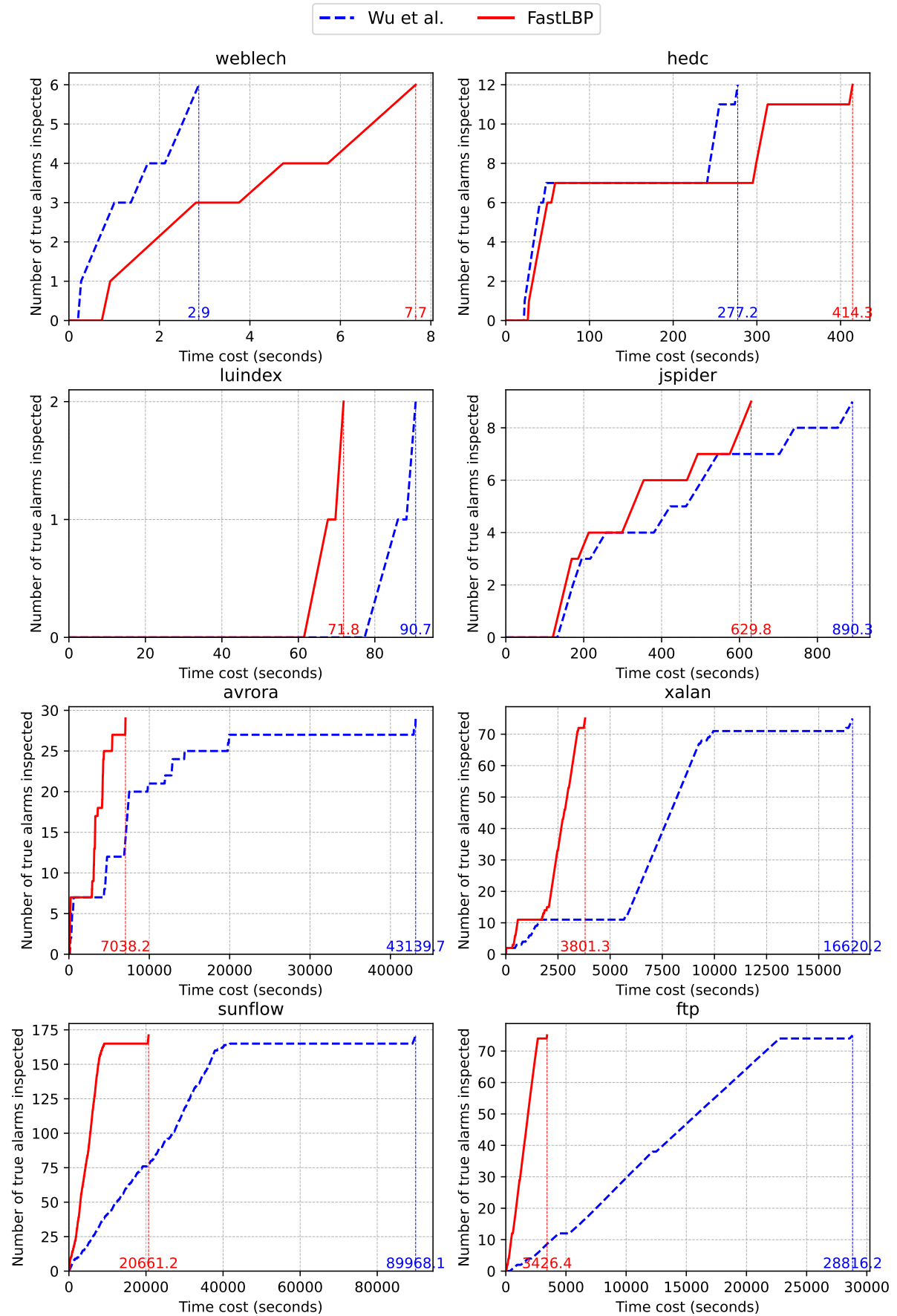


Figure 8: Comparison of execution time between Wu et al. and FastLBP.

fixed number of iterations, this experiment adopts PARALL as the update strategy for both methods, with the number of iterations fixed at 200.

**Accuracy.** Table 8 summarizes the results of three accuracy metrics. Compared to PGMax, FastLBP achieves average improvements of  $-7.89\%$ ,  $-1.52\%$ , and  $-16.18\%$  in Rank-100%-T, Rank-90%-T, and Inversion, respectively. Overall, FastLBP exhibits slightly higher accuracy than PGMax, primarily due to higher numerical precision in its results. One contributing factor is that FastLBP uses double-precision floating-point arithmetic, whereas PGMax uses single precision. Another factor is that FastLBP incorporates numerical error reduction techniques from the library [7], leading to more accurate inference outcomes. We also present the ROC curves in Figure 9. On the majority of benchmarks, FastLBP achieves a larger AUC. Only on a few benchmarks does PGMax outperform FastLBP. Indeed, minor deviations from our law are inevitable, as differences in numerical precision can influence the Bayesian program analysis process, either positively or negatively. In aggregate, however, FastLBP demonstrates slightly superior accuracy compared to PGMax.

Table 8: Accuracy for PGMax and FastLBP. OOM (out of memory) indicates that PGMax exceeded the GPU memory capacity during execution. In such cases, data could not be collected or compared fairly, and these entries are therefore excluded from the table. The average relative change is the arithmetic mean of individual relative changes.

Benchmark	Rank-100%-T		Rank-90%-T		Inversion	
	PGMax	FastLBP	PGMax	FastLBP	PGMax	FastLBP
weblech	11	11	11	11	22	23
hedc	152	69	151	66	642	458
luindex	162	233	162	233	320	462
jspider	257	230	257	230	1,269	469
avrora	915	631	741	624	7,697	7,043
xalan	447	586	246	338	5,507	6,307
sunflow	OOM	748	OOM	425	OOM	38,632
ftp	415	274	204	185	8,277	1,942
Average Change Rate	7.89% $\downarrow$		1.52% $\downarrow$		16.18% $\downarrow$	

**Execution Speed.** Figure 10 shows the number of true alarms identified over time by PGMax and FastLBP. On all benchmarks, FastLBP identifies all true alarms in less time than PGMax. This performance advantage stems from FastLBP’s incorporation of the optimization based on Horn clauses for LBP proposed by Wu et al. (Section 2.3), whereas PGMax performs message passing computation using Equation (2). When computing a message from a factor to a variable, FastLBP achieves linear complexity with respect to the number of neighboring variables, while PGMax incurs exponential complexity. As a result, FastLBP is consistently more efficient than PGMax across all benchmarks. Table 9 provides detailed data on total and average execution time. Compared to PGMax, FastLBP achieves speedups of  $5.56\times$  in total execution time and  $4.78\times$  in average execution time. In summary, FastLBP outperforms the state-of-the-art GPU-based parallel method in terms of execution speed.

## 6 Related Work

There has been extensive research on accelerating LBP, and this section provides a summary of related work.

**Methods Based on Local Structure.** Wu et al. [31] proposed a method to accelerate LBP by exploiting local structures [8]. The core idea is to encode factors in the factor graph using if-then-else statements, thereby simplifying the representation of factor functions and reducing the computational complexity of message passing in LBP. The factors considered in this work exhibit a special form of local structure—Horn clauses—which can be viewed as a specific instance of their framework. In contrast to this prior work, our contribution lies in the parallelization of LBP for such structured factors, enabling efficient GPU-based execution.

**GPU-Accelerated Methods.** GPU-based acceleration of LBP has been applied in various domain-specific contexts, such as computer vision [15, 5] and error-correcting codes [28]. This work aims to

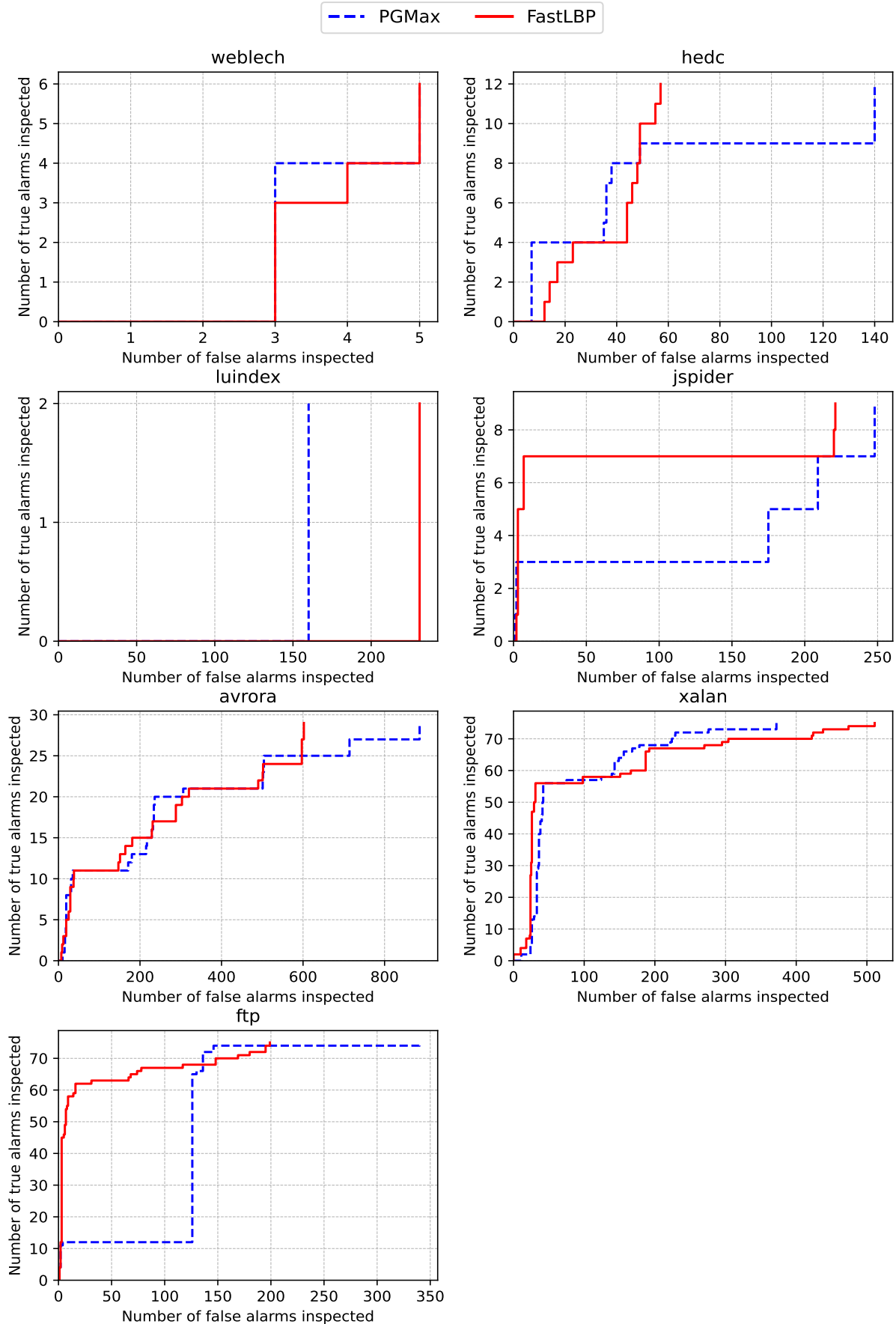


Figure 9: Comparison of ROC curves between PGMax and FastLBP.

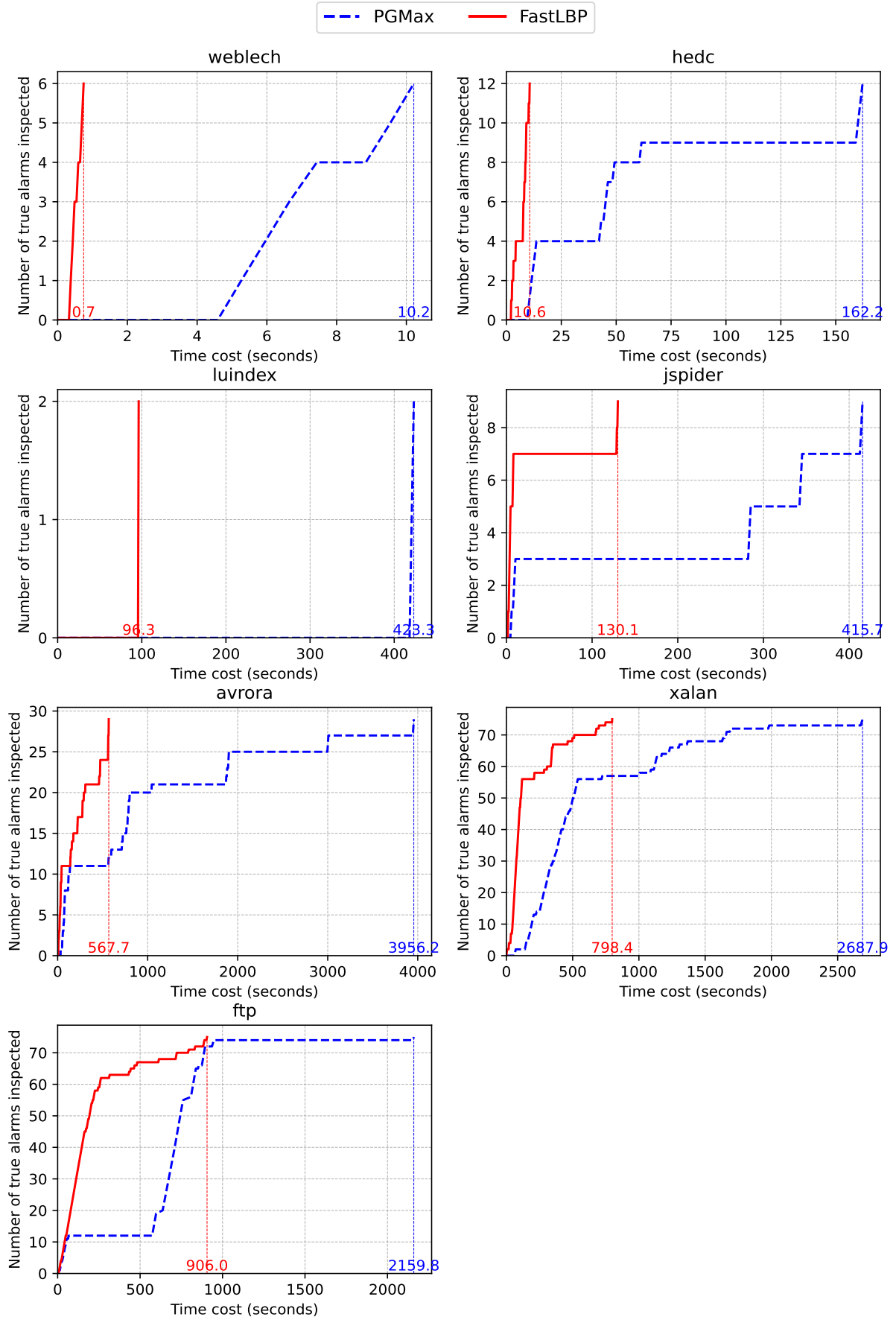


Figure 10: Comparison of execution time between PGMax and FastLBP.

Table 9: Execution time for PGMax and FastLBP. The meaning of OOM is the same as in Table 8. The average speedup is the geometric mean of individual speedups.

Benchmark	Total Execution Time (s)		Average Execution Time (s)	
	PGMax	FastLBP	PGMax	FastLBP
weblech	10.21	0.75	0.93	0.07
hedc	162.22	10.61	1.07	0.15
luindex	423.28	96.31	2.61	0.41
jspider	415.69	130.08	1.62	0.57
avrona	3956.16	567.70	4.32	0.90
xalan	2687.95	798.36	6.01	1.36
sunflow	OOM	2369.02	OOM	3.17
ftp	2159.81	905.99	5.20	3.31
Average Speedup	5.56 $\times$		4.78 $\times$	

accelerate LBP in the context of program analysis using GPUs. Compared to these prior efforts, our approach deals with probabilistic graphical models that are significantly larger in scale and more complex in structure, as well as different types of local structures. Beyond domain-specific applications, Zhou et al. [38] implement LBP using JAX [4], enabling GPU acceleration for general-purpose LBP. In contrast to their work, our method supports sophisticated update strategies and is specifically optimized for special local structure of Horn clauses.

Another body of related work focuses on system-level optimizations [33, 30, 18, 14]. These approaches exploit characteristics of computer vision tasks to optimize memory usage and bandwidth utilization, and to efficiently leverage registers and shared memory for improved performance. However, due to the more irregular and complex graph structures prevalent in program analysis, the techniques from these works cannot be directly transferred to our setting. While system-level optimization is not the primary focus of this paper, exploring deeper optimizations on top of our method remains a promising direction for future research.

**Scheduling Strategies for Message Passing.** This work focuses specifically on scheduling strategies for message passing on GPUs. Romero and Chang [29] designed a specialized parity-check matrix for LDPC codes to enable LBP to retain the benefits of sequential updating while exploiting GPU parallelism. However, this approach is limited to LDPC code decoding. In contrast, our method also strikes a balance between parallelism and sequential updating, but is applicable to arbitrary probabilistic graphical models.

Several other approaches [9, 13, 20] are designed for general LBP. Residual Belief Propagation [9] introduces the concept of residual and updates the most influential messages in parallel during each iteration, aiming to accelerate convergence. Residual Splash [13] extends the residual idea from edges to vertices, selecting a set of vertices with the highest residuals and propagating updates in a breadth-first manner to a certain depth. Randomized Belief Propagation [20] randomly selects a subset of messages to update in each iteration, effectively balancing convergence behavior and parallel efficiency. Our work is orthogonal to these methods. On the one hand, they can be integrated with our parallel framework to further improve performance or convergence. On the other hand, these prior works primarily evaluate their effectiveness in terms of execution speed and convergence behavior on specific datasets, e.g., computer vision. Their applicability and effectiveness in the context of program analysis remain to be investigated.

## 7 Conclusion and Future Work

Loopy Belief Propagation (LBP) has been widely applied in computer science, and improving its computational efficiency is of significant importance. This work presents a GPU-accelerated LBP algorithm tailored for program analysis. To support diverse update strategies, we model each strategy as a strict partially ordered set over the edges of the factor graph, enabling uniform dependency analysis for message updates. To achieve parallel acceleration on probabilistic graphical models with special local structures, our method groups different types of message computations into batches for efficient execution. Experimental results demonstrate that our approach achieves an average speedup of 2.14 $\times$  over the state-of-the-art sequential method and 5.56 $\times$  over the state-of-the-art GPU-based parallel method, while maintaining

equivalent accuracy in inference outcomes.

The method of this work can still be developed. Currently, the set of supported update strategies is limited. Future efforts could explore integrating update strategies designed for other domains into our framework, and evaluating whether such extensions lead to better results.

## References

- [1] Serge Abiteboul, Richard Hull, and Victor Vianu. *Foundations of Databases: The Logical Level*. Addison-Wesley Longman Publishing Co., Inc., USA, 1st edition, 1995. ISBN 0201537710.
- [2] Reid Morris Bixler. *Sparse matrix belief propagation*. PhD thesis, Virginia Tech, 2018.
- [3] Stephen M. Blackburn, Robin Garner, Chris Hoffmann, Asjad M. Khang, Kathryn S. McKinley, Rotem Bentzur, Amer Diwan, Daniel Feinberg, Daniel Frampton, Samuel Z. Guyer, Martin Hirzel, Antony Hosking, Maria Jump, Han Lee, J. Eliot B. Moss, Aashish Phansalkar, Darko Stefanović, Thomas VanDrunen, Daniel von Dincklage, and Ben Wiedermann. The dacapo benchmarks: java benchmarking development and analysis. *SIGPLAN Not.*, 41(10):169–190, October 2006. ISSN 0362-1340. doi: 10.1145/1167515.1167488. URL <https://doi.org/10.1145/1167515.1167488>.
- [4] James Bradbury, Roy Frostig, Peter Hawkins, Matthew James Johnson, Chris Leary, Dougal Maclaurin, George Necula, Adam Paszke, Jake VanderPlas, Skye Wanderman-Milne, and Qiao Zhang. JAX: composable transformations of Python+NumPy programs, 2018. URL <http://github.com/jax-ml/jax>.
- [5] A. Brunton, Chang Shu, and G. Roth. Belief propagation on the gpu for stereo vision. In *The 3rd Canadian Conference on Computer and Robot Vision (CRV'06)*, pages 76–76, 2006. doi: 10.1109/CRV.2006.19.
- [6] Tianyi Chen, Kihong Heo, and Mukund Raghethaman. Boosting static analysis accuracy with instrumented test executions. In *Proceedings of the 29th ACM Joint Meeting on European Software Engineering Conference and Symposium on the Foundations of Software Engineering*, ESEC/FSE 2021, page 1154–1165, New York, NY, USA, 2021. Association for Computing Machinery. ISBN 9781450385626. doi: 10.1145/3468264.3468626. URL <https://doi.org/10.1145/3468264.3468626>.
- [7] Yifan Chen, Yiqian Wu, and Xin Zhang. libdai. <https://github.com/Neuromancer42/libdai>, 2024.
- [8] Professor Adnan Darwiche. *Modeling and Reasoning with Bayesian Networks*. Cambridge University Press, USA, 1st edition, 2009. ISBN 0521884381.
- [9] Gal Elidan, Ian McGraw, and Daphne Koller. Residual belief propagation: informed scheduling for asynchronous message passing. In *Proceedings of the Twenty-Second Conference on Uncertainty in Artificial Intelligence*, UAI'06, page 165–173, Arlington, Virginia, USA, 2006. AUAI Press. ISBN 0974903922.
- [10] Mahdi Eslamimehr and Jens Palsberg. Race directed scheduling of concurrent programs. *SIGPLAN Not.*, 49(8):301–314, February 2014. ISSN 0362-1340. doi: 10.1145/2692916.2555263. URL <https://doi.org/10.1145/2692916.2555263>.
- [11] Tom Fawcett. An introduction to roc analysis. *Pattern recognition letters*, 27(8):861–874, 2006.
- [12] Pedro F. Felzenszwalb and Daniel P. Huttenlocher. Efficient belief propagation for early vision. *Int. J. Comput. Vision*, 70(1):41–54, October 2006. ISSN 0920-5691. doi: 10.1007/s11263-006-7899-4. URL <https://doi.org/10.1007/s11263-006-7899-4>.
- [13] Joseph Gonzalez, Yucheng Low, and Carlos Guestrin. Residual splash for optimally parallelizing belief propagation. In David van Dyk and Max Welling, editors, *Proceedings of the Twelfth International Conference on Artificial Intelligence and Statistics*, volume 5 of *Proceedings of Machine Learning Research*, pages 177–184, Hilton Clearwater Beach Resort, Clearwater Beach, Florida USA, 16–18 Apr 2009. PMLR. URL <https://proceedings.mlr.press/v5/gonzalez09a.html>.

[14] Scott Grauer-Gray and John Cavazos. Optimizing and auto-tuning belief propagation on the gpu. In *Proceedings of the 23rd International Conference on Languages and Compilers for Parallel Computing*, LCPC’10, page 121–135, Berlin, Heidelberg, 2010. Springer-Verlag. ISBN 9783642195945.

[15] Scott Grauer-Gray, Chandra Kambhamettu, and Kannappan Palaniappan. Gpu implementation of belief propagation using cuda for cloud tracking and reconstruction. In *2008 IAPR Workshop on Pattern Recognition in Remote Sensing (PRRS 2008)*, pages 1–4, 2008. doi: 10.1109/PRRS.2008.4783169.

[16] Daphne Koller and Nir Friedman. *Probabilistic Graphical Models: Principles and Techniques - Adaptive Computation and Machine Learning*. The MIT Press, 2009. ISBN 0262013193.

[17] F.R. Kschischang, B.J. Frey, and H.-A. Loeliger. Factor graphs and the sum-product algorithm. *IEEE Transactions on Information Theory*, 47(2):498–519, 2001. doi: 10.1109/18.910572.

[18] Chia-Kai Liang, Chao-Chung Cheng, Yen-Chieh Lai, Liang-Gee Chen, and Homer H. Chen. Hardware-efficient belief propagation. In *2009 IEEE Conference on Computer Vision and Pattern Recognition*, pages 80–87, 2009. doi: 10.1109/CVPR.2009.5206819.

[19] David JC MacKay and Radford M Neal. Near shannon limit performance of low density parity check codes. *Electronics letters*, 32(18):1645–1646, 1996.

[20] Mark Van der Merwe, Vinu Joseph, and Ganesh Gopalakrishnan. Message scheduling for performant, many-core belief propagation. In *2019 IEEE High Performance Extreme Computing Conference (HPEC)*, pages 1–7, 2019. doi: 10.1109/HPEC.2019.8916366.

[21] Ana Milanova, Atanas Rountev, and Barbara G. Ryder. Parameterized object sensitivity for points-to analysis for java. *ACM Trans. Softw. Eng. Methodol.*, 14(1):1–41, January 2005. ISSN 1049-331X. doi: 10.1145/1044834.1044835. URL <https://doi.org/10.1145/1044834.1044835>.

[22] Joris M. Mooij. libdai: A free and open source c++ library for discrete approximate inference in graphical models. *Journal of Machine Learning Research*, 11(74):2169–2173, 2010. URL <http://jmlr.org/papers/v11/mooij10a.html>.

[23] Kevin P. Murphy, Yair Weiss, and Michael I. Jordan. Loopy belief propagation for approximate inference: an empirical study. In *Proceedings of the Fifteenth Conference on Uncertainty in Artificial Intelligence*, UAI’99, page 467–475, San Francisco, CA, USA, 1999. Morgan Kaufmann Publishers Inc. ISBN 1558606149.

[24] Mayur Naik. Chord: A program analysis platform for java, 2006. URL <https://bitbucket.org/psl-lab/jchord/src/master/>.

[25] NVIDIA Corporation and affiliates. Sparse matrix formats, 2024. URL [https://docs.nvidia.com/nvpl/latest/sparse/storage\\_format/sparse\\_matrix.html](https://docs.nvidia.com/nvpl/latest/sparse/storage_format/sparse_matrix.html).

[26] Judea Pearl. *Probabilistic Reasoning in Intelligent Systems: Networks of Plausible Inference*. Morgan Kaufmann Publishers Inc., San Francisco, CA, USA, 1988. ISBN 1558604790.

[27] Mukund Raghethaman, Sulekha Kulkarni, Kihong Heo, and Mayur Naik. User-guided program reasoning using bayesian inference. In *Proceedings of the 39th ACM SIGPLAN Conference on Programming Language Design and Implementation*, PLDI 2018, page 722–735, New York, NY, USA, 2018. Association for Computing Machinery. ISBN 9781450356985. doi: 10.1145/3192366.3192417. URL <https://doi.org/10.1145/3192366.3192417>.

[28] Bharath Kumar Reddy L. and Nitin Chandrachoodan. A gpu implementation of belief propagation decoder for polar codes. In *2012 Conference Record of the Forty Sixth Asilomar Conference on Signals, Systems and Computers (ASILOMAR)*, pages 1272–1276, 2012. doi: 10.1109/ACSSC.2012.6489228.

[29] David L. Romero and Nicholas B. Chang. Sequential decoding of non-binary ldpc codes on graphics processing units. In *2012 Conference Record of the Forty Sixth Asilomar Conference on Signals, Systems and Computers (ASILOMAR)*, pages 1267–1271, 2012. doi: 10.1109/ACSSC.2012.6489227.

- [30] Vibhav Vineet and P. J. Narayanan. Cuda cuts: Fast graph cuts on the gpu. In *2008 IEEE Computer Society Conference on Computer Vision and Pattern Recognition Workshops*, pages 1–8, 2008. doi: 10.1109/CVPRW.2008.4563095.
- [31] Yiqian Wu, Yifan Chen, Yingfei Xiong, and Xin Zhang. Belief propagation with local structure and its applications in program analysis. In *Proceedings of the 40th IEEE/ACM International Conference on Automated Software Engineering*, ASE ’25. Association for Computing Machinery, 2025. To appear.
- [32] Yiqian Wu, Yujie Liu, Yi Yin, Muhan Zeng, Zhentao Ye, Xin Zhang, Yingfei Xiong, and Lu Zhang. Smartfl: Semantics based probabilistic fault localization. *IEEE Transactions on Software Engineering*, 51(7):2161–2180, 2025. doi: 10.1109/TSE.2025.3574487.
- [33] Qingxiong Yang, Liang Wang, Ruigang Yang, Shengnan Wang, Miao Liao, and David Nister. Real-time global stereo matching using hierarchical belief propagation. In *Bmvc*, volume 6, pages 989–998. Citeseer, 2006.
- [34] Chen Yanover and Yair Weiss. Approximate inference and protein-folding. In S. Becker, S. Thrun, and K. Obermayer, editors, *Advances in Neural Information Processing Systems*, volume 15. MIT Press, 2002. URL [https://proceedings.neurips.cc/paper\\_files/paper/2002/file/100d9f30ca54b18d14821dc88fea0631-Paper.pdf](https://proceedings.neurips.cc/paper_files/paper/2002/file/100d9f30ca54b18d14821dc88fea0631-Paper.pdf).
- [35] Muhan Zeng, Yiqian Wu, Zhentao Ye, Yingfei Xiong, Xin Zhang, and Lu Zhang. Fault localization via efficient probabilistic modeling of program semantics. In *2022 IEEE/ACM 44th International Conference on Software Engineering (ICSE)*, pages 958–969, 2022. doi: 10.1145/3510003.3510073.
- [36] Xin Zhang, Radu Grigore, Xujie Si, and Mayur Naik. Effective interactive resolution of static analysis alarms. *Proc. ACM Program. Lang.*, 1(OOPSLA), October 2017. doi: 10.1145/3133881. URL <https://doi.org/10.1145/3133881>.
- [37] Yifan Zhang, Yuanfeng Shi, and Xin Zhang. Learning abstraction selection for bayesian program analysis. *Proc. ACM Program. Lang.*, 8(OOPSLA1), April 2024. doi: 10.1145/3649845. URL <https://doi.org/10.1145/3649845>.
- [38] Guangyao Zhou, Antoine Dedieu, Nishanth Kumar, Wolfgang Lehrach, Shrinu Kushagra, Dileep George, and Miguel Lázaro-Gredilla. Pgmax: Factor graphs for discrete probabilistic graphical models and loopy belief propagation in jax. *Journal of Machine Learning Research*, 25(371):1–25, 2024. URL <http://jmlr.org/papers/v25/23-1010.html>.